Received: 20 April 2023 | Revised: 3 October 2023 | Accepted: 5 October 2023

DOI: 10.1002/esp.5734

CASE STUDY

ESPL WILEY

# The internal structure of spring mounds of Nefzaoua oasis in Tunisia: Formation of an original geomorphic structure

Afef Raddadi[1] | Pascal Podwojewski[2]

[1]UMR ARCHEORIENT Environnements et Sociétés de l'Orient ancien, UMR 5133, Université Lumière Lyon 2, Lyon cedex 7, France

[2]UMR IEES-Paris, IRD, SU, INRAE, CNRS, UP, UPEC, IRD, Bondy cedex, France

**Correspondence**
Pascal Podwojewski, UMR IEES-Paris, IRD, SU, INRAE, CNRS, UP, UPEC, IRD, delegation régionale Île de France, 32 av. H. Varagnat, 93143 Bondy cedex, France.
Email: pascal.podwojewski@ird.fr

**Funding information**
French laboratory "Archéorient-Environnements et sociétés de l'Orient Ancien", Grant/Award Number: UMR 5133; IRD (UMR IEES-Paris)

## Abstract

Spring mounds are specific geomorphological landforms in arid or semi-arid environments associated with playas and artesian springs. Spring mounds are found worldwide, especially in the great Artesian Basin of Australia and in North American and Egyptian deserts. They result from an exceptional succession of climatic, geomorphological and hydrogeological conditions, with processes that follow each other in a specific order. In Tunisia, in the arid zone, ca. 126 spring mounds have been identified in Nefzaoua province alone, especially in the oasis east of Chott el Jerid. They have a conical shape that ranges from 200 to more than 2000 m in diameter and 3–30 m tall, and their centre is hollowed out by an artesian spring of fresh water. Palm groves (*Phoenix dactylifera*) spread out at the foot of each mound. The springs have dried up because of the proliferation of borehole wells. Because of the low electric conductivity (EC) of the sediments (<1 mS $cm^{-1}$) at their base, spring mounds have been excavated and used as a soil amendment to expand new palm plantations. This excavation allows for analysis of their internal structure, which has never been observed well. In the present study, fine analysis of sediment layers in four sections of two representative mounds showed that vegetation had trapped sediment at their base. Fine strata of variable texture alternating with variable calcium carbonate, gypsum or organic carbon contents suggest a clear limnic origin. Many redoximorphic features, sometimes associated with the presence of old roots, suggest variation in the water level in the centre of the mound. The mounds are capped by a thick layer of indurated gypsum, which helps them resist hydric and aeolian erosion. The origin of the sediment components is discussed.

**KEYWORDS**
anthropic degradation, geomorphic structure, oases, spring mound, Tunisia

## 1 | INTRODUCTION

Spring mounds are geomorphological landforms associated with artesian springs that emerge from the soil surface and have been described in a large variety of environments and with different lithological composition. In semi-humid climate in South Africa, mounds are made with peat (McCarthy et al., 2010). Mounds occur in hydrothermal volcanic environments, such as in Bolivia (Bougeault et al., 2019) or in Ethiopia and Djibouti (Fontes & Pouchan, 1975) where they are made with pure limestone. In hyper-arid oases in Egypt (Brookes, 1993; Idris, 1996; Powell & Fensham, 2015; Torab, 2014, 2021), many mounds are recovered by iron oxide deposits protecting them from erosion (Adelsberger & Smith, 2010). In Mediterranean environment in Spain, Pellicer et al. (2014) described the mounds as tufa mound complex. In the semi-arid south-western United States (USA), mounds are associated with playas (Blinn et al., 1994; Neal & Motts, 1967), made with algal tufa and cyanobacteria (Scholl, 1960; Scholl & Taft, 1964). Some are recovered with

a gypsum cap in Tunisia (Roberts & Mitchell, 1987) and in Syria (Besançon et al., 2000). The larger distribution of spring-mounds occurs in Australia, specifically its Great Artesian Basin (Clarke et al., 2007; Harris, 1981; Ponder, 1986; Powell et al., 2015; Watts, 1973). The mounds lithological compositions are complex (Ponder, 1986) constructed of autochthonous materials precipitated by the spring waters quartz sand and clay and minor carbonate deflated from the hinterland and trapped in the vicinity of the spring by vegetation (Clarke et al., 2007), After Keppel et al. (2011), carbonate deposits were interpreted to be largely plant or microbial tufa, while Franchi & Frisia (2020) interpreted the formation of carbonates precipitated in extreme, continental environments by biotic and abiotic complex mechanisms of crystallization. Recent studies compared them with features of the Martian landscape (Clarke et al., 2007; Essefi et al., 2014; Ori, 2010; Pellicer et al., 2014).

In Tunisia, Jones and Millington (1986) first mapped an alignment of small spring mounds using remote sensing in northern Nefzaoua province, in south-western Tunisia, in the playa of the *Chott Fjedj* (Figure 1a and b). Later, Roberts & Mitchell (1987) documented many more spring mounds east of the *Chott El Jerid*, the largest playa in northern Africa. Australia has more than 600 springs in an area of the Great Artesian Basin (1.7 million km$^2$) (Ponder, 1986) and more than 60 active springs in the Dalhousie Mound Spring Complex (Clarke et al., 2007), but there is no clear indication of the internal organization of these mounds or how they developed. In Tunisia, in Nefzaoua province alone, south of Djebel Tabagha in an area of 3000 km$^2$, more than 126 spring mounds have been clearly identified (Raddadi, 2021; Raddadi et al., 2021). The size of only 88 mounds could be determined with a larger diameter ranging between 250 and 2430 m (average 877 ± 465 m) and an altitude ranging between 2 and 28 m (average 12 ± 5 m) (Raddadi & Podwojewski, 2022a). The mounds are associated with oases east of the *Chott El Jerid* (Figure 1C). Spring mounds have lain at the centre of all permanent oasis settlements in Nefzaoua province for more than 2000 years, and all current oasis plantations there radiate around them (Figure 2).

Some mounds in Nefzaoua province have been mechanically excavated (Raddadi et al., 2021; Raddadi & Podwojewski, 2022a), which completely revealed their internal structure in vertical sections

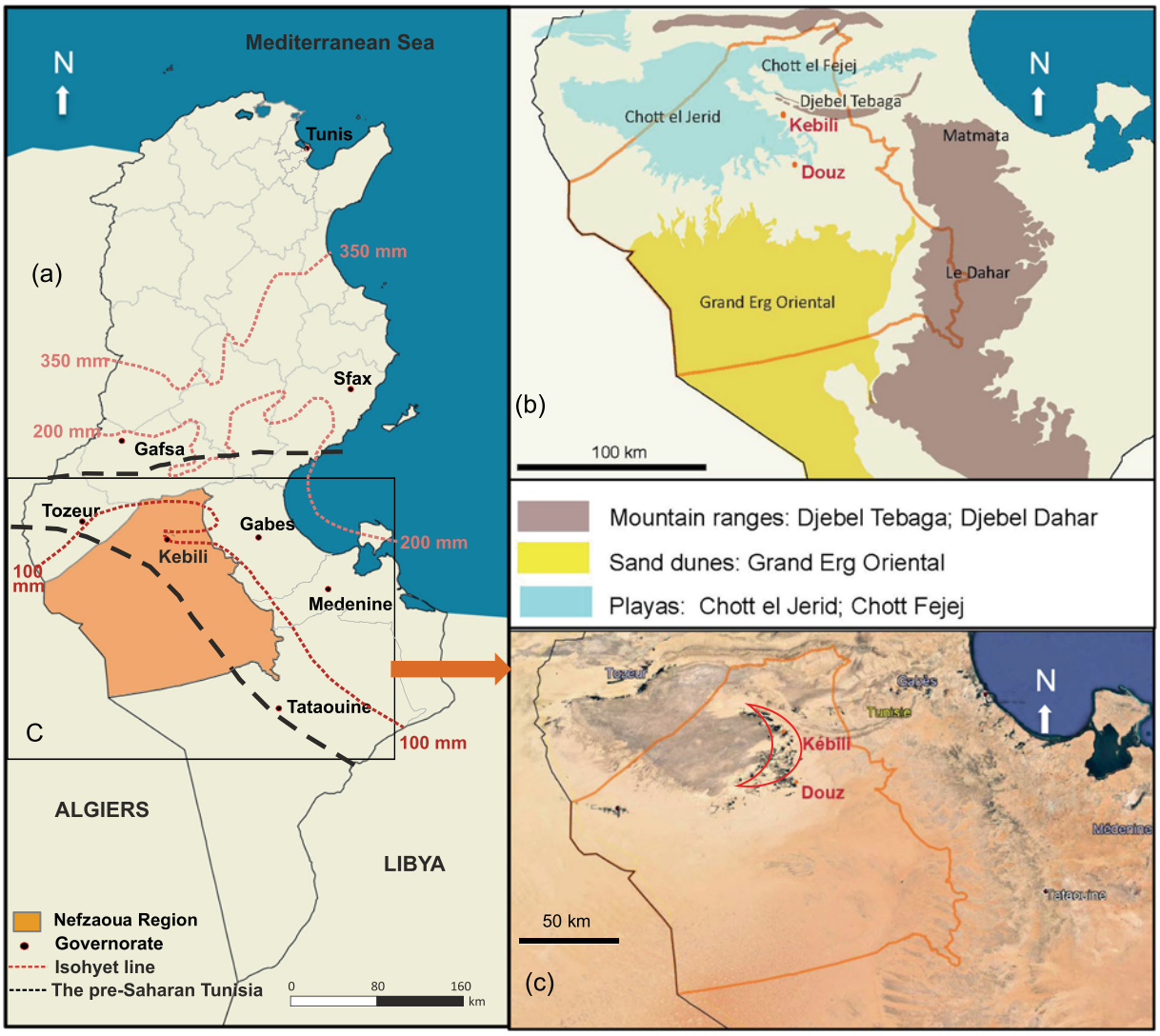


**FIGURE 1** (a) Location of the Nefzaoua region (Governorate of Kebili in South West Tunisia) and the limit of the presaharian Tunisia. (b) Location of the cities of Kebili and Douz at the centre of the four geomorphological units: Djebel Dahar and Djebel Thebaga mountain ranges, Chott El Jerid playa and grand erg oriental sand dunes (c) Detail of Figure 2A, satellite image of the set of oases in a crescent shape east of the playa of the Chott El Jerid. Limit of the Nezaoua region in orange. [Color figure can be viewed at wileyonlinelibrary.com]


**FIGURE 2** Satellite image of a spring mound without vegetation close to the city of Blidet (red square), west of Douz and east of *Chott El Jerid* (C), with radiating palm tree plantations at the foot of the mounds. Inside the yellow circle: the study site of sections a, B and C (Figure 5). Inside limit 1: individual spring mound; inside limit 2: coalescent spring mounds (Raddadi, 2021). [Color figure can be viewed at wileyonlinelibrary.com]

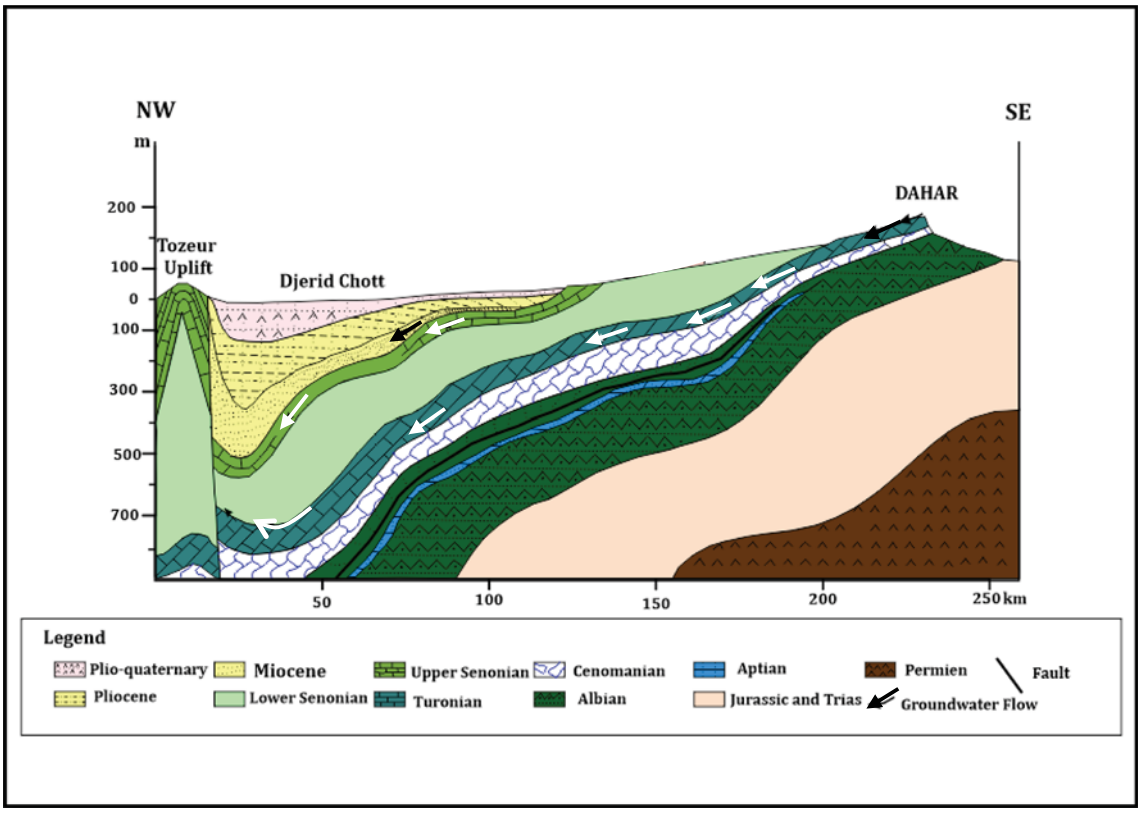


**FIGURE 3** Hydrogeological cross section of *Complexe terminal* aquifers (Hadj Ammar et al., 2014). [Color figure can be viewed at wileyonlinelibrary.com]

and thus provided a unique opportunity for the present study's stratigraphical and pedological analysis. These mounds are representative of a semi-desert environment with no volcanic nor hydrothermal influence, in the vicinity of very large saline endorheic playas. The aim of this study is to describe the internal structure of these mounds, to explain the lithological variation of sedimentary strata with a complex

mixture of aeolian quartz sand deposits associated with carbonates and gypsum, and to suggest different hypothesis for the origin and the evolution of these layers.

## 2 | INTRODUCTORY MATERIAL

### 2.1 | Geological and geomorphological contexts

Tunisia, the smallest country of the Maghreb, is split in its centre into northern and southern parts by a vast synclinal oriented east–west that is filled by a set of flat evaporitic playas called *sebkha: Chott Fjej* and *Chott El Jerid* (Figure 1B). In the north, the Atlas massif was formed during the Alpine orogenesis, while the southern part is located in the Saharan platform (Coque, 1962). The Nefzaoua province in south-western Tunisia corresponds to the governorate of Kebili. It is located at the junction of two anticlinal domes – Fjej and Dahar – in a synclinal subsident depression (Figure 3). These two domes are fractured by a transforming fault that remains active (Swezey, 1996). Thus, the province lies at the crossroad of four landforms (Figure 1B):

- In the north, the Cretaceaous monoclinal structure of the *Djebel Tebagha* mountain chain culminates at 470 m asl, is oriented east–west, and has a dip oriented to the south. It consists of layers of different sedimentary rocks, mainly limestone, dolomite, gypsum and mudstone:
- In the east, the piedmont of the monoclinal Jurassic structure of *Djebel Dahar* culminates at 713 m asl, is oriented north–south, and has a dip with a gentle slope oriented to the west. It also consists of layers of different sedimentary rocks, mainly limestone, dolomite, gypsum and mudstone;
- Large sand dunes of the *Grand Erg Oriental* to the south-west;
- The vast depression of *Chott El Jerid* in the west. The playa covers more than 5860 km$^2$ and is ca. 15 m asl; it is the largest endorheic playa in Africa.

### 2.2 | Hydrogeological context

Southern Tunisia has two captive fossil water tables. The deeper aquifer dates mainly to the lower Cretaceous (from Neocomian to Albian stages) (the *Continental intercalaire* [CI] formation), while the shallower water table dates to the Senonian stage, with sub-horizontal layers from the Miocene to the present (the *Complexe terminal* [CT] formation) (Figure 3). These two aquifers are separated by an impermeable layer of clays, mudstones and siltstones that date to the Albian-Cenomanian stages (OSS, 2003). These water tables cover a vast area of 1 million km$^2$ from the southern Algerian Atlas chain to western Libya (Gonçalvès et al., 2013). This area also contains shallow aquifers recharged by the infrequent rainfall on the recharge zones.

The groundwater flow lines converge mostly towards the *Chott Jerid* with a slope of the geological layers oriented to the north-west. The piezometric gradient observed in the Dahar chain decreases consistently towards *Chott Jerid*, indicating the importance of this chain in the recharge of shallow aquifers (Kraiem et al., 2014). The Tebaga chain is also a secondary recharge zone. The *Chott Jerid* and the south-western Dahar piedmont at Douz are the natural discharge areas of these shallow aquifers (Haj-Amor et al., 2017). Groundwater from boreholes in this area has a low-to-moderate salt content (total dissolved solids: 600–3700 mg l$^{-1}$); the cationic water composition is dominated by $Ca^{++}$ (68–941.3 mg l$^{-1}$) and $Na^{+}$ (77.9–1357.2 mg l$^{-1}$), the anionic composition is dominated by $Cl^{-}$ (135.4–2775.3 mg l$^{-1}$) and $SO_4^{2-}$ (141.6–2307.7 mg l$^{-1}$), (Hadj Ammar et al., 2014). Water mineralization is regulated mainly by water-rock interactions through mineral dissolution and likely by ion exchange with a long residence time (Hadj Ammar et al., 2014; Kraiem et al., 2014). Evaporite deposits in the *sebkhas* have no direct influence on the chemical composition of the main water tables (Hadj Ammar et al., 2014; Kraiem et al., 2014).

### 2.3 | Weather conditions

The region has a hot desert climate (BWh in the Köppen classification), with mean rainfall less than 100 mm yr$^{-1}$ (less than 80 mm yr$^{-1}$ in the past 20 years). The little rain that falls from September–April has large inter-annual and inter-monthly variability. Some rainfall events heavier than 20 mm can occur, which generate runoff.

The mean annual temperature is 20.9°C, with extreme daily, monthly and seasonal amplitudes. Maximum temperatures during the dry summer can exceed 48°C, while minimum temperatures during the winter can become negative (−5°C) at night. The calculated annual evapotranspiration exceeds 1600 mm, with a strong water deficit.

In these arid environments, wind is the main cause of erosion and geomorphological agent. Most strong winds come from the north-east and east-north-east. From April–July, 40% of the winds measured in Kebili exceed 3 m s$^{-1}$ (Figure 4; data from the Tunisian National Meteorological Office; Khatelli & Gabriels, 2000).

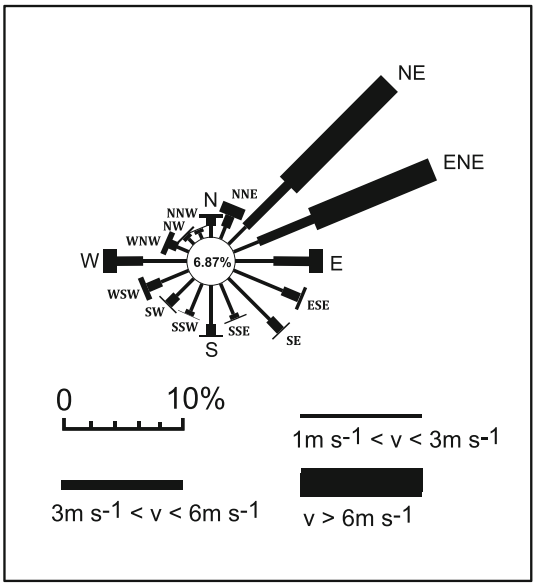


**FIGURE 4** Wind rose and wind speed (V) at the Kebili weather station.

### 2.4 | Human settlement

Evidence of human settlement since the Neolithic period has been found in the Nefzaoua province. Some Roman-era traces (i.e., irrigation canals called *seguia*, which translates as "tunnels" or "collectors") testify to the presence of a developed agricultural system based on irrigation around the springs (called *aïoun*) (Trousset, 1986). The irrigated agricultural system, from a partially nomadic to a completely sedentary population, was sustained by maintaining the infrastructure and regularly cleaning the province's ca. 300 natural artesian springs (Lasram, 1990; Sghaier, 1999). In the past 40 years, because of the development of solar-powered water pumps, the area of irrigated intensive palm tree plantations (*Phoenix dactilifera*) increased from 5000 to 20 000 ha (Raddadi, 2021) and all artesian springs disappeared; in addition, the spring mounds have no longer been sustained by regular flooding since 1995 (Marlet et al., 2009; Zammouri et al., 2007). Following the decrease in the water table level, the spring mounds naturally silted up and eroded or were artificially levelled (Raddadi & Podwojewski, 2022a). Because the sediments of spring mounds have low electrical conductivity (EC) values at their base, which means low salt contents, many of them have recently been excavated to extend palm-tree plantations beyond the salty edges of the *chott* (Raddadi, 2021; Raddadi et al., 2021; Raddadi & Podwojewski, 2022a). Their mechanical destruction has exposed their internal structure as vertical sections.

### 2.5 | Spring mounds studied

Of the 126 spring mounds in the area, two were selected because they showed a complete and continuous vertical section, which many levelled or excavated mounds do not show. The excavations of spring mounds clearly revealed fine stratification and the lateral and vertical organization at their heart. The layers showed high vertical variability in colour and texture for fine sampling for further analysis. A total of 86 sediment samples were collected: 62 in four sections (A, B, C and D) and 24 samples from three soil cores augered to a depth of 1.6 m, with one sample every 20 cm (i.e., eight samples per core).

## 3 | METHODS

### 3.1 | Section sampling

The larger spring mound is located in the Aïn Chardiouss oasis near Blidet (TRT 36, Raddadi & Podwojewski, 2022b), south of the city of Kebili (Figures 2 and 5). It was nearly 750 m in diameter, 16 m tall (Raddadi, 2021) and almost completely excavated and dismantled by heavy machinery. Three sections were sampled: one complete section north of the spring (section A, 34 samples more than 13 m tall, 33° 34′ 21″ N, 8° 50′ 25″ E), and two partial sections south of the spring (section B, nine samples 33°34′16″ N, 8°50′26″ E) and on the external part of the mound (section C, 33°34′16″N, 8°50′19″ E). Two soil cores were augured: one (T1) in the centre, near the probable spring and one (T2) near section C. Because section A was 13 m tall, it was sampled using a crane with a basket, from the top down, as for a standard soil profile.

The second spring mound Ouled Aïssa (TRT 9, 33° 42′ 27″ N, 8° 53′ 51″ E, Raddadi & Podwojewski, 2022a) west of Kebili, is one of the few in a good state of preservation. It is 500 m in diameter and 8 m tall (Raddadi & Podwojewski, 2022b). Only the external part of the spring mound is excavated (Figure 6) and described as section D, with 11 samples. One soil core was augured in the centre of the structure. The spring mound, described by Roberts & Mitchell (1987), has an oval shape oriented north-east to south-west 150 m long, 50–80 m wide and 5–10 m tall, divided by a small valley 5–10 m wide. At

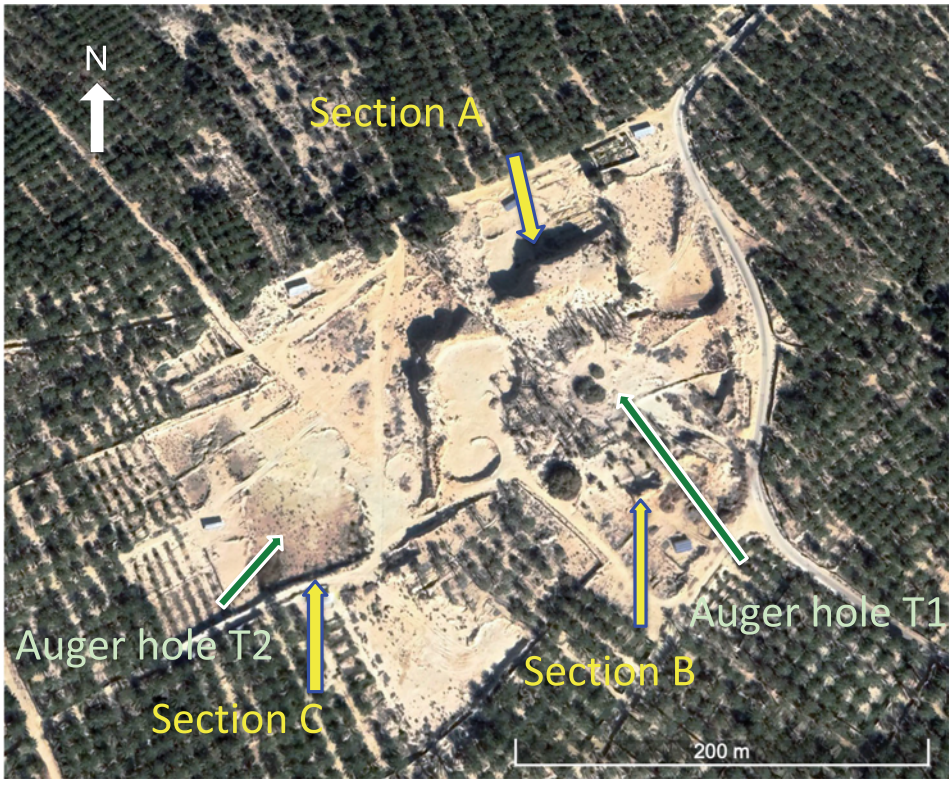


**FIGURE 5** Locations of sections A, B and C and core samples T1 and T2 of spring mound TRT 36. See also Figure 2). [Color figure can be viewed at wileyonlinelibrary.com]

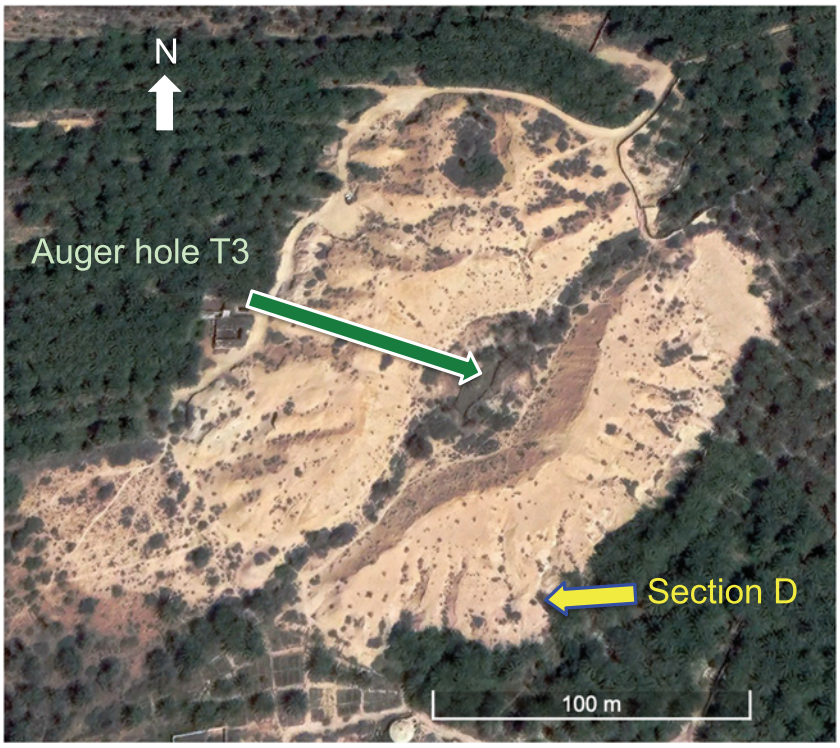


**FIGURE 6** Location of section D and core sample T3 of spring mound TRT 9. [Color figure can be viewed at wileyonlinelibrary.com]

the centre of the valley, traces of the former spring and some palm trees indicate the origin of irrigation channels from the spring through the valley.

## 3.2 | Analytical methods

Nearly all of the 86 samples had the consistency of a soft to moderately indurated sediment. The samples were air dried, sieved and then analysed at the water and soil laboratory of the Institute of Arid Regions (Medenine, Tunisia), using the methods of Pansu & Gautheyrou (2006) for determining calcium carbonate and gypsum contents. The soil organic carbon (SOC) content was measured using the Walkley–Black method (Walkley, 1947). Carbonate content was determined using a pressure calcimeter, and gypsum content was determined by gravimetry (precipitation with $BaCl_2$). Sediment pH was measured in a 1:2.5 soil: water solution, and EC was measured using a conductimeter in a 1:5 soil: water solution. Because the standard method of creating a saturated paste is time consuming, we estimated the influence of salinity when it exceeded 2000 µS $cm^{-1}$ (2 dS $m^{-1}$), which corresponds to the concentration of a solution saturated in gypsum. For this, we used the local correction of Aboukila & Abdelaty (2017) specifically adapted for sandy soils:

$$EC_{sat} = EC_{1:5} \times 7.46 - 0.43 \quad (1)$$

A salic horizon (if soil pH ≤ 8.5) has an EC with saturated paste >15 dS $m^{-1}$ (IUSS, WRB, 2022), which corresponds, after the equation (1), to an $EC_{1:5}$ of ca. 2 mS $cm^{-1}$. Soil texture was determined by dry sieving with a set of 16 sieves from 1600 to 50 µm with a logarithmic progression. The dry sieving allowed the size of air-blown particles to be quantified for this region of strong aeolian erosion and sedimentation because it emphasizes the amount of coarse agglomerated particles. Determining clay and silt contents by wet sieving after dispersal with hexametaphosphate and a pipette is not suitable for gypsum layers and needs many adaptations (Vieillefon, 1979). Therefore, the texture of sediments that clearly contained gypsum was not determined by wet sieving.

### 3.2.1 | Micro-analysis

The morphology of some aggregates was analysed using an electron microscope (Zeiss Evo®, Carl Zeiss Ltd., UK) with an acceleration voltage of 15 kV and magnification of up to 10,000×. It was coupled with a DRX microprobe with dispersal energy (INCA Energy 350 EDX, Oxford Instruments, UK). The clay mineralogy of specific samples was determined for the fraction smaller than 2 µm in diameter. Samples were analysed using an X-Ray Diffractometer (Siemens D500) with Ni-filtered CuKα radiation at 40 kV and 30 mA. Oriented air-dried, glycolated and heated (500°C for 3 h) samples were scanned from 2°–15° (2θ), with measurement for 2 s every 0.02°. For some samples, the fraction smaller than 2 µm was also prepared as a randomly oriented powder mount and scanned from 2 to 70° (2θ).

# 4 | RESULTS

Descriptions of all sections (Figure S1) and analytical results were summarized by Raddadi & Podwojewski (2022c) (Table S1).

## 4.1 | Section A

Section A was 13 m tall on the largest excavated profile (Figure 7). It had regular horizontal stratification of 34 identified fine sedimentary

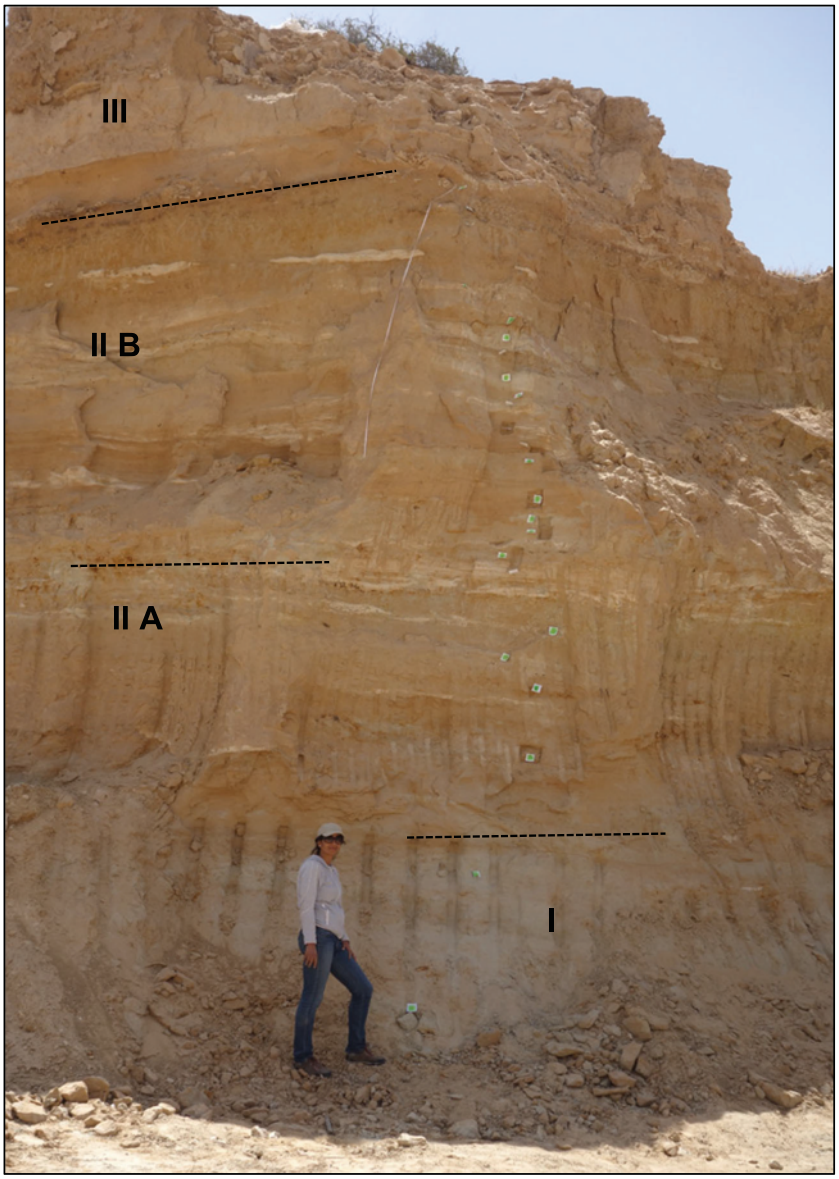


**FIGURE 7** Photograph of section A, with boundaries between major units. [Color figure can be viewed at wileyonlinelibrary.com]

sub-horizontal layers from the top to its base (Figure 8). The profile was divided into three major units.

The base unit (I) extended from 9.40 to 13.00 m deep (samples A30 and A31). The base was built on fine aeolian deposits with a large dominance of fine sands (80–100 μm) (Figure S1A and B), which are characteristic of aeolian deposits (Chepil, 1951a). At the base of this profile, the layers were homogenous, with no particular sign of strata, with a pale yellow colour (5Y5/2) typical of a reduced environment. The layers contained almost no SOC, some carbonates (< 4%) and almost no gypsum (≥0.4%) and had a very low EC (>0.35 mS $cm^{-1}$).

The intermediate unit (II) had two compartments: IIA, with five layers (A25–A29) 7.40–9.40 m deep, and IIB, with 17 layers (A8–A24) 3.15–7.40 m deep. They represented two major sedimentary subdivisions, with sharp changes in texture and high variability in EC. The boundary between compartments A and B was sharp. The thin 5 cm thick layer showed evidence of reticular dark reddish (2.5YR 5/6) and black features (Figure S8 C). Manganese (Figure S6 C to E) and iron oxides (Figure S6 F to J) were identified as cutanic deposits on quartz grains.

The lower part of compartment IIB (A19–A23), has a low EC and fine sands, while the upper compartment (A8–A18), composed of very fine centimetric strata, many of them enriched in carbonates and coarse sand. This level also showed evidence of hydromorphic redoximorphic features of a pale grey colour (10YR 6/3 and 10YR 7/3), and strong brown mottles (10YR 5/6 and 10YR 6/6) generally associated with fluctuation of high and lower carbonate and SOC contents with no direct link. The top layers of compartment IIB (A8–A11) were gypsiferous and had a high EC (2.4–7.7 mS $cm^{-1}$).

The upper unit (III) (0–3.20 m deep) had no redoximorphic features. It consisted of a fine aeolian sand layer with low EC (A6–A7 < 2.4 mS $cm^{-1}$) low gypsum and carbonate contents covered by a gypsic hardpan (A1–A3). Some human artefacts were found in this layer (e.g., animal bones, potsherds, flint arrowheads).

## 4.2 | Section B

Section B consisted mainly of aeolian deposits (Figures S2 and S3) and had no gypsum layer on the top. The base unit (I) consisted of fine sand (layers B1–B5) (2.80–5.00 m deep) of a light brown colour (10YR 6/4) with low EC (<1 mS $cm^{-1}$). Base layer B1 (4.00–5.00 m deep) was interesting in that it consisted of thin centimetric to millimetric

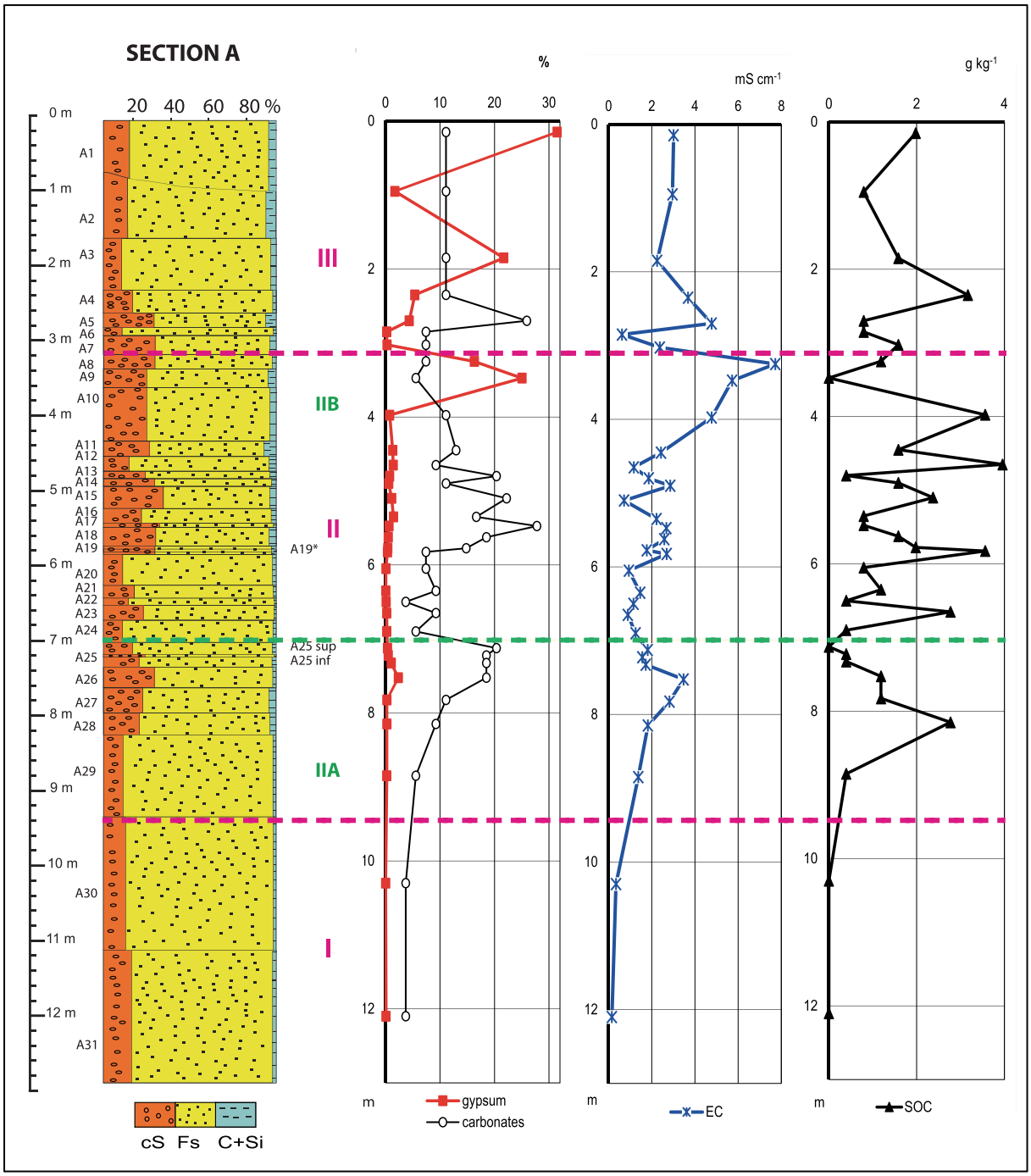


**FIGURE 8** Section A. Variation in texture: cS: coarse sand (2000–200 µm), fS: fine sand (200–50 µm), C + Si: clay+silt (<50 µm), gypsum and carbonate contents (%), electrical conductivity (EC) (mS $cm^{-1}$), and soil organic carbon (SOC) (mg $kg^{-1}$). [Color figure can be viewed at wileyonlinelibrary.com]

layers of sand enriched in SOC (Figure 13A). Unit II (layers B6 and B7) (2.40–2.80 m deep) had higher EC (>3.0 mS $cm^{-1}$) and was enriched in coarse sand and some gypsum. The top layers (unit III) were sandy, with low EC (<1.0 mS $cm^{-1}$) and a low gypsum content.

## 4.3 | Section C

Section C was short but had three units (Figures S4 and S5). Base unit I (layers CI–C3) (1.30–2.00 m deep) had very low EC (>0.2 mS $cm^{-1}$), low SOC content and small redoximorphic features. In a clay extraction of layer C2, four types of clay were identified by XRD determination (i.e., kaolinite, illite, smectite and palygorskite, Figure S7 C2). The intermediate unit (II) (layers C4–C6) (0.60–1.20 m) had a lower clay content, higher EC (>1.0 mS $cm^{-1}$) and was enriched in carbonates (≥14%). The top unit (III), enriched in gypsum, was typical of all spring-mounds of the Nefzaoua province.

Section D was 5.5 m tall (Figure 9) and had regular horizontal stratification of 11 sedimentary sub-horizontal layers divided into three major units (Figure 10). The fine strata of unit II were grouped into thicker layers.

The base unit (I) (layers D1–D3) (4.80–5.30 m deep) consisted of pale brown fine sand (10YR 7/3) enriched in carbonates (>20%) and with a low EC (<1.2 mS $cm^{-}1$). Layer D2 was enriched in SOC. The intermediate unit (II) consisted of two sedimentary compartments – D3–D4 (3.50–4.80 m deep) and D6–D9 (1.50–3.80 m deep)

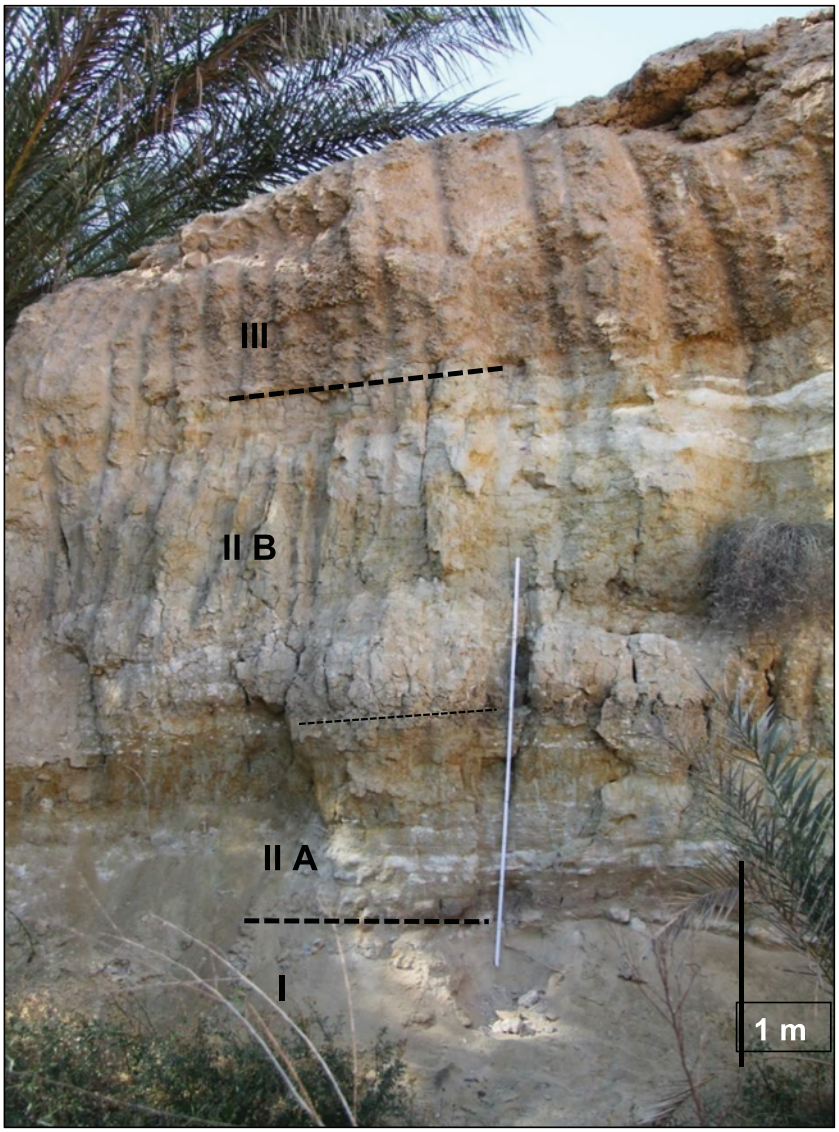


**FIGURE 9** Photograph of section D, with boundaries between major units. [Color figure can be viewed at wileyonlinelibrary.com]

– beginning with a clayey base. In a clay extraction in layer D6, four types of clay similar to those observed at the base of section C were identified by XRD determination (i.e., kaolinite, illite, smectite, palygorskite and traces of chlorite) (Figure S6 Q to X; Figure S7 D6). The layers show evidence of redoximorphic features, with clear root presence in a gleyic horizon (IUSS-WRB, 2022) (Figure 13 B and C) and higher EC (>2 mS $cm^{-1}$). The top unit (III) consisted of sandy aeolian deposits enriched in gypsum. The top of the profile was a calcrete and gypsic hardpan resistant to aeolian erosion. A gypsum crust (<1 cm) as a skin in thin layers covered part of the vertical excavated section surface (Figure S8 A and C).

### 4.4 | Auger soil cores

All three auger soil cores (Table S1) had a relatively homogenous composition at each sampling site. All had low EC at the base (≤0.8 mS $cm^{-1}$ for T1 and T2 and ≤1.8 mS $cm^{-1}$ for T3) that increased toward the soil surface (>2.1 mS $cm^{-1}$), which corresponded to an increase in carbonate and gypsum contents. The SOC content was also much higher than that of mound sediments; many layers exceeded 0.8% SOC. Profile T1 had the highest variability in SOC content (0–9.1 g $kg^{-1}$) and was sandy (mostly fine sand) and light brown in colour. T2, away from the spring, had much more clay (>20%) and coarse sand (>20%), and a typical reduced colour (5Y 7/3). T3 was darker (10YR 3/3), with higher SOC (7.3–12.9 g $kg^{-1}$) and a texture similar to that of T1 but with more coarse sand.

## 5 | DISCUSSION

The history of the Nefzaoua spring-mounds can be divided into four phases: i) development of a water table with artesian springs; ii) establishment of vegetation around a spring, which traps aeolian sand and initiates formation of a mound, iii) sediment deposition and iv) pedogenesis in the sediments.

### 5.1 | Development of a water table with artesian springs

The geomorphologic conditions for the first phase consist of three steps (Figure 11, steps 1 to 3). As mentioned, natural recharge of the water tables in this area converges at the lowest elevation of

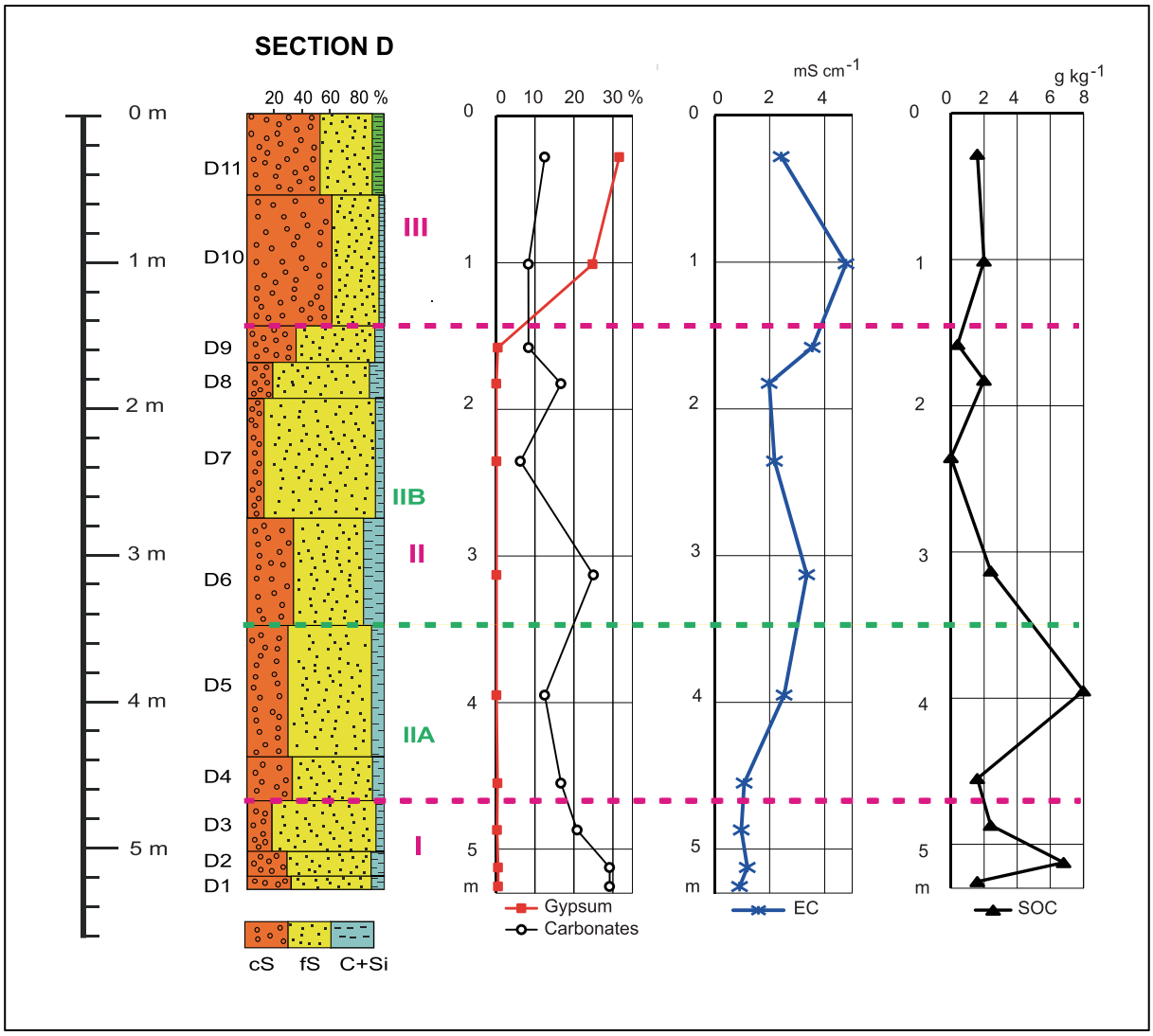


**FIGURE 10** Section D. Variation in texture: cS: coarse sand (2000–200 µm), fS: fine sand (200–50 µm), C + Si: clay+silt (<50 µm), gypsum and carbonate contents (%), electrical conductivity (EC) (mS $cm^{-1}$) and SOC (mg $kg^{-1}$). [Color figure can be viewed at wileyonlinelibrary.com]

the endoreic basin of *Chott El Jerid* (maximum of +15 m). The recharge zone is mainly the Dahar chain, with a west-facing slope, followed by the Tebaga chain, with a south-facing slope. As in many other regions with desertic artesian springs, low playas (in southern California (Scholl, 1960; Neal & Motts, 1967), endoreic basins or flat depressions (Ponder, 1986) (in western Egypt (Powell & Fensham, 2015)), the spring mounds of the Nefzaoua basin are located in flat areas and associated with artesian systems (Coque, 1962; Pouget, 1968). Some aligned micro springmounds were described by Essefi et al. (2014), in the Sidi El Habi sebkha in the north east Tunisia as direct consequence of groundwater upwelling triggered by tectonics and hydraulics. Swezey (1996) suggested that alignment of mounds near the Chott el Jerid resulted from neotectonic activity and faults with emerging artesian springs.

## 5.2 | Colonization by vegetation

After geomorphologic, climatic and tectonic conditions generate artesian springs, the second phase of formation of a spring mound is colonization by vegetation around the spring and entrapment of drifting sand (Figure 12 steps 4 and 5; Adelsberger & Smith, 2010). All mound bases in that area were built mainly on fine sand (80–100 µm), which is characteristic of aeolian deposits (Chepil, 1951b; Table S1; Figure S6A, B). The local vegetation consists of a steppe of shrubs and grasses (Asteraceae and Poaceae) less than 0.5 m tall and with less than 50% of soil cover (Le Houerou, 1959). In Tunisia, studies by Bendali et al. (1990) showed the role of two plants in trapping sand: *Rhanterium suaveolens* (Asteraceae), in the least disturbed areas, and *Stipagrostis pungens* (Poaceae), in wind corridors. These species can maintain the density of their structures after sand accumulates, in part by constantly renewing adventitious roots, which provide them with water from reserves in the accumulated sand. These plants are associated with *nebkas*, dunes in the process of forming, and are able to create sand hillocks up to 2 m tall called *rebdou* (Coque, 1962). The hillocks contain alternating layers of sand and organic matter under the plants. Essefi et al. (2014) described this early stage process of formation associating vegetal entrapment of aeolian particles in some embryonic and child age of some young Tunisian spring mounds.

All Nefzaoua spring mounds were formed over sand trapped by vegetation forming mounds. These features are visible at the base of the external part of the spring mounds, such as in section B

| | | |
|---|---|---|
| 1 | **The filling of the watertables**: The rain water is collected from two monoclinal sedimentary structures through natural impluvium. The structure of the Djebel Tabagha is oriented East-West, which dip is oriented to the south and the Djebel Dahar is oriented North-South, which dip presents a gentle slope oriented to the West. | 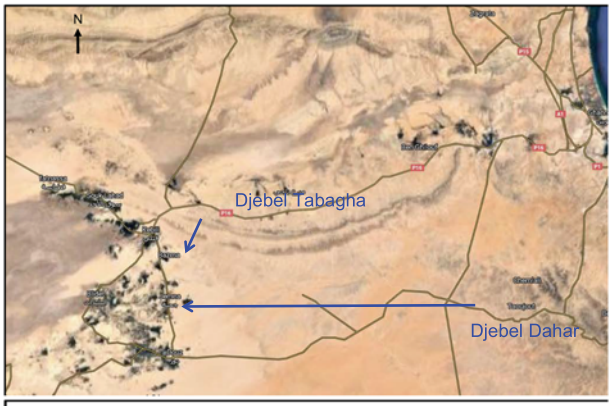  |
| 2 | **Water-table with pressure**: The piezometric level of the watertable is located above the soil surface. The rain-water is trapped in a porous layer between two impermeable levels above and below it. | 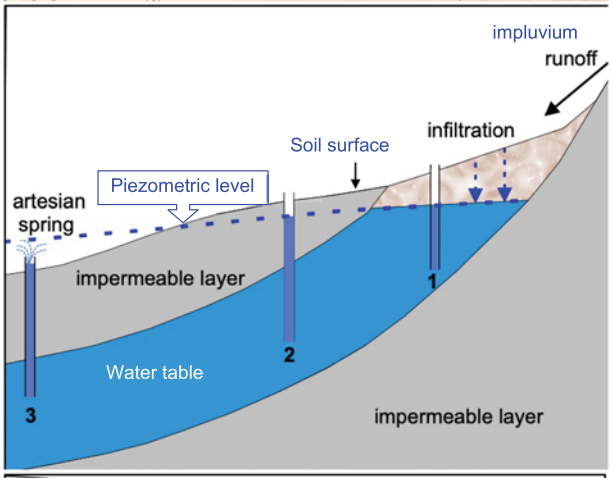  |
| 3 | **Tectonic, compression**: when a fault occurs between the layer at the top of the watertable and the soil surface, the mineral water emerge from the water table with pressure. This spring is qualified as artesian because of its natural gushing. | 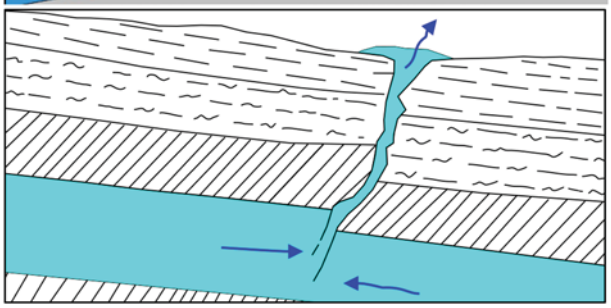 |

**FIGURE 11** Steps of spring mound formation: the artesian process step 1: the filling of the water tables; step 2: water-table with pressure and step 3: tectonic, compression. [Color figure can be viewed at wileyonlinelibrary.com]

(I) (Figure 13A) or layer D2. These layers had higher SOC content than the other layers (7.2 and 6.8 g $kg^{-1}$, respectively), which was confirmed by the high SOC content in many of the soil core layers (up to 9.1, 8.3 or 12.9 g $kg^{-1}$ in T1, T2 and T3, respectively) (Table S1). These dunes constitute the elevated edge of the ponds that form close to the artesian spring.

## 5.3 | Filling of the pond and lacustrine deposits

When water collects and the pond expands, many processes occur. The pond expands to the boundary formed by the dunes that are set by vegetation, and then sediment accumulates (Figure 12 steps 6 and 7). The frequent variation in layer thickness, the slight variation in texture and colour because of the degree of oxidation–reduction and the different accumulation forms of calcium carbonates (§ chapter below) suggest a complex combination of processes linked to the fluctuation of the water level in the pound. Sedimentation depends on the following factors:

i. *Variation in spring discharge*, which determines the amount of water in the pond. This discharge is likely influenced by climatic variations and the contribution of higher annual rainfall during the Palaeocene and Holocene (Swezey, 2003). During the Holocene, paleo lakes in the Sahara desert experienced periods of higher rainfall (7500–9500 and 4500–5500 yrs ago), with drier phases in between (Guo et al., 2000). In Egypt, spring mounds were associated with human settlements during the early wet Holocene, until the settlements disappeared in the post-Roman period (Adelsberger & Smith, 2010; Bravard et al., 2016).
ii. *Variation in sediment inputs*, which are almost exclusively aeolian because spring mounds are elevated and experience little contamination from external sediment flows during high rainfall events. The sediments consisted almost exclusively of aeolian rounded quartz grains with homometric size of 80–100 μm in diameter (Figure S6A and B), with features of impacts in V shape (Figure S6 E) (Niftah et al., 2005). The coarse fraction contained micro-grains of quartz cemented with carbonates and/or gypsum

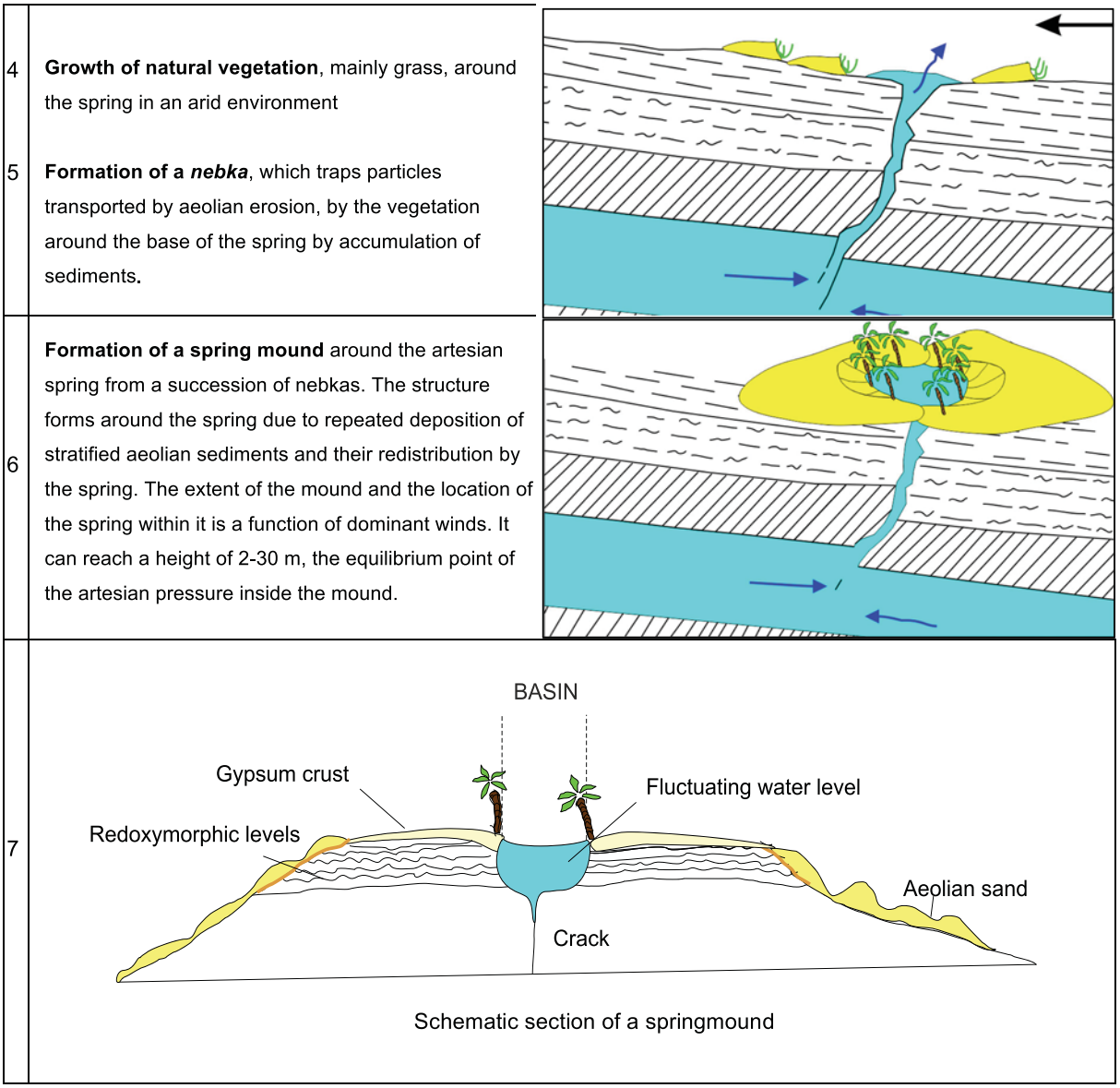


**FIGURE 12** Steps of spring mound formation. Steps 4 and 5: growth of natural vegetation; formation of a nebka; step 6: formation of a spring mound; step 7: schematic section of a spring-mound. [Color figure can be viewed at wileyonlinelibrary.com]

(Trichet, 1963), not individual coarse sand grains. The same features are observed in the Jeffara plain to the east (Jouquet et al., 2021). However, we observed no micro-evidence of biogenic formation of tufs or gypsum constructions (Stivaletta & Barbieri, 2009. We also did not observe laminar-deposit structures such those observed in the *sebkha*. As suggested by Schulz et al. (2002) and Barbieri et al. (2006), these milimetric layers of bacteria and algae can trap and retain dust and fine-grained matter.

iii. *Variation in spring chemistry* due to local variation in the chemical composition of the water table. It is often associated to previous rainfall events. All of the springs have dried up, sedimentation is no longer visible, and the water chemistry is no longer measured. Because the chemical composition of the water determines which minerals precipitate, (Williams & Holmes, 1978), it is difficult to estimate the inputs of precipitated salts (e.g., carbonates or sulphates). It is also difficult to estimate the proportions of inputs of precipitated salts and inputs of sedimentary particles (e.g., feldspar sands and clays) released from the aquifer, which were transported vertically though geological layers by the ascending spring water,

## 5.4 | Evolution of the sediments, pedogenic processes

### 5.4.1 | Clay mineralogy

The clay types and the XRD peaks were absolutely similar in two different sections (C and D) corresponding to two different layers of two different mounds located 17 km apart (Figure S7). The mineralogical composition was similar to those found in different soil surveys in the *chott* region of eastern Algiers, in the same geomorphological and climatological environment in the regions of Touggourt (Djoughi & Semra, 2017) and Ouargla (Youcef, 2016). The origins of these clay types (Dixon & Weed, 1989) suggest a strong variation of climatic

conditions with rainy periods (neoformation of kaolinite), drier environments (neoformation of smectite), inherited (Illite) and wind-blown fibrous clays from playa environments (palygorskite). Because clays particles are coated on quartz grain, they can be easily transported by the wind and formed in different environments (Figure S6 K, L, Q to X).

### 5.4.2 | Redoxymorphic features

The sediment layers are submitted to pedogenetic processes such as oxydo-reduction often processes associated with the presence of root traces (Figure 13, step 8B and C). Some mounds such as TRT 22 (not studied, Figure S8A) or section A (Figure 13, 8B) show layers with evidences of gleyic features at their base with pale yellow colour 5Y 8/2 to 2.5Y 7/4 (claric feature) associated with strong brown mottles (7.5 to 10YR 5/8) around the root traces indicating a fluctuation of a water-table as an upward moving agent (IUSS-WRB, 2022). In the same section of TRT 22 (Figure S8A and B) and in the level 4 of section D, (Figure 13, 8C) stagnic features with filling of pale yellow colour (5Y 7/2 to 7/3) around vertical root traces in strong brown matrix (7.5YR 5/8). Stagnic properties are caused by stagnation of an intruding agent (in that case emerging spring-water) that causes reducing conditions. It leads to an overlying Fe-poor layer and an underlying layer with oximorphic features (IUSS-WRB, 2022). Mobilized Mn (Figure S6C, D and E) in black mottles and Fe oxides (Figure S6H, I and J) in red mottles (10R4/8) may precipitate at the base of these level such as the level 25 section A (Figure S8C). This is suggesting phases of relative fast building of the mound with evidences of submersion alternating with phases of pedogenesis after air-drying and oxidation with internal fluctuation of a water-table and precipitation of carbonates and sulphates.

### 5.4.3 | Accumulation of carbonates

Some springs in hydrothermal conditions in Ethiopia and Djibouti (Fontes & Pouchan, 1975) or Bolivia (Bougeault et al., 2019) develop calcareous travertines and tufs, which have also been described in the USA (Scholl, 1960), Spain (Pellicer et al., 2014), Egypt (Adelsberger & Smith, 2010) and Australia (Clarke et al., 2007; Ponder, 1986) using biosignatures (Franchi & Frisia, 2020; Keppel et al., 2011).

In our stratigraphic layers, however, the main component was an aeolian fine sand with homometric quartz grains, potentially cemented by powdery carbonates in 2 μm crystals (Figure S6M and N). Carbonates accumulate in various features (Figure 13, step 9) sometimes form powdery massive layers (Figure 13D) considered as groundwater calcretes or palustrine primary carbonate mud cemented (Alonso-Zarza, 2003) as a chalky horizon (Alonso-Zarza & Wright, 2010). Vertical decimetric concretions are looking like root moulds in palustrine environment (Figure 13E). Hard nodules of various shapes, are aligned (Figure S8A, some have platy shape of 5 cm high and 20–30 cm long, looking like desiccation cracks in palustrine environment (Figure 13F). No biological features, such as travertines of tufs, were noted in the carbonate samples in the sections studied. As carbonates precipitates often in relation of plant root and biological activity, the different shapes of calcium carbonate accumulation suggest a precipitation in shallow fluctuating water level associated with redoxymorphic features with evidences of vegetal roots. Further investigations are needed to associate the different origins of carbonate features with biological activity and their depositional environment.

### 5.4.4 | Accumulation of gypsum

Gypsum clearly accumulated on top of the spring mounds (Figure 13 step 10). These accumulations were more than 50 cm thick in profiles A and D. They were indurated as a gypsum crust (Figure S8D), as described by Pouget (1968), Watson (1985, 1988) and Stivaletta & Barbieri (2009) and may have resulted from two different accumulation processes:

i. *Leaching from aeolian sediments*, as suggested by Coque (1962) to explain the alignment of mounds considered as fossil sand dunes. Since then, White & Drake (1993), Drake et al. (1994) and Drake (1997) used geomorphological, archaeological and remote-sensing data to support the aeolian erosion of gypsiferous sediments. The sediments came from the Fjej *sebka*, located leeward to the north-east of the spring mound area, and were consolidated by rainfall following deposition. This accumulation suggested strong segregation of particles by the wind. Gypsum (bulk density of 2.30 g $cm^{-3}$) could be transported in coarser grains more easily than sand (bulk density of 2.65 g $cm^{-3}$). By tracing gypsum origins using isotopic $\delta^{34}S$ analysis, Drake et al. (2004) suggested that gypsiferous bedrock influences the long-term preservation of crusts by providing a replenishing source or by promoting saturation of surface runoff and thus reducing the runoff's ability to dissolve other gypsiferous matter.

Aspects of this theory have been questioned by Watson (1985, 1988), who suggested that aeolian gypsum is mobilized by meteoric waters and leached down-profile, where it is subsequently deposited. These subsurface crusts may later be exhumed by deflation to form surficial crusts.

However, the accumulation of aeolian gypsum by deflation occurs only leeward at the footslope North of the Tebagha range (Drake, 1997). In our case the gypsum dunes described by Coque (1962) are not randomly distributed such as sand dunes where the crests are exposed to the wind and moving with time, but are restricted to the top of the discontinuous sets of spring mounds in relation with tectonic faults. They never show a classical *barkhane* sand dune shape visible in the Grand Erg Oriental South West of the Chott el Jerid. Such aeolian concentration of gypsum sands is therefore unlikely to occupy only the top of the mounds.

ii. *Evaporation*, such as in a *sebkha* with a stable pond level (Figure S6O and P). Bureau and Roederer (1960) suggested that the bedrock provides the source, and that *capillary rise* of soil water transports calcium and sulphate to the surface, where they precipitate. Thus, the gypsum accumulates on the top edge of a mound strata in equilibrium with the artesian pressure for a long period. The horizontal strata of the sediments are a discontinuity in pore connectivity, and the rise cannot exceed 2 m because of the fine silt texture (Li et al., 2018; Lu & Likos, 2004), where the rise is assumed to be constant. Pouget (1968) suggested


8 A) evidence of fine organic strata alternating with sand sedimentation; (B) vertical oxidized root traces in a reduced environment (gleyic features); (C) vertical reduced root traces in an oxidized environment (stagnic features).


9 D) Section A level 25, precipitation of $CaCO_3$ in powdery layers; E) Indurated vertical carbonates accumulations Looking as root moulds; F) platy aligned indurated concretions, desiccation cracks? Gypsum coating (Gy) from dissolution of gypsum top-crust and precipitation over the section.

9 Precipitation of $CaCO_3$ in powdery layers, pockets, nodules and concretions between sediment layers;

10 Formation of a gypsum crust (Gy) at the top of the mound likely due to capillary rise and some aeolian inputs.

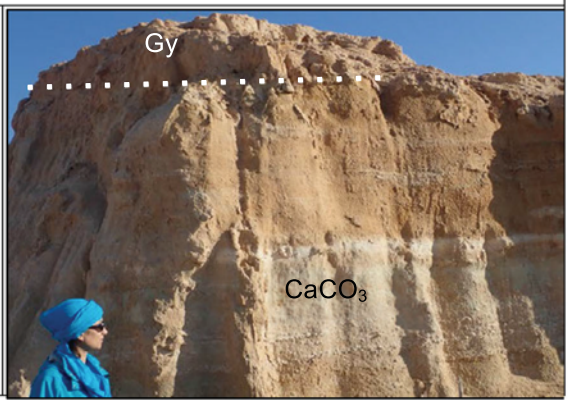


**FIGURE 13** Steps of spring mound formation; step 8: soil development and redoxymorphic processes: step 9: neoformation of calcium carbonate accumulation of different shapes: Step10: accumulation of gypsum forming a crust at the top of the spring mound. [Color figure can be viewed at wileyonlinelibrary.com]

precipitation because of capillary rise of saline water associated with input of soft water, which decreases $Cl^-$ contents and lessening the product of solubility of the gypsum, which precipitates.

In the specific case of the gypsum occurrence in the Tunisian spring mounds, we agree with the suggestion of Watson (1985) "the geomorphological significance of this model of gypsum crust genesis cannot be overstated with certainty". However, we suggest the following process:

i. The EC concentration increases from the base to the top of the mound indicating a probable origin *per ascensum* from a water table. No sign of stratification was visible in the gypsum cap. It suggests that when the pressure of the spring was at its maximum, the mound stops its growth and evapotranspiration could redistribute the salts at the surface.
ii. During further scarce heavy rainfall events, gypsum particles are partially dissolved at the top of the mound and leached and a *per descensum* cementation occurs during dry period. Very recent

gypsum deposits leached from the top of the mound (Figure 13 F; Figure S8A and C) are deposited as a skin over many excavated vertical sections. This occurrence is therefore very rapid. The erosion of free gypsum particles with Aeolian erosion of the topsoil is likely and the occurrence of the gypsic hardpan at the top of mostly all spring mounds will protect the mounds from further aeolian and hydric erosion. After Monaco et al. (2020), the archaeological settlements studied in the Nefzaoua province East of the city of Douz, −2000 BC for the oldest, are all located on top of the gypsum crust.

## 6 | CONCLUSION

The excavation of Tunisian spring mounds allowed their internal structure to be described and analysed. It is organized in three general units: i) at the base, fine organic layers alternating with fine sand, suggesting entrapment by vegetation with inputs from aeolian erosion; ii) fine limnic centimetric layers, with increasing EC from the base to the top, with alternating colours depending on the carbonate content, and redoximorphic features, with traces of former roots; and iii) a gypsic hardpan 1.0 m thick on the top, with no evidence of sedimentation.

This structure confirms the succession of processes that form spring mounds: i) natural recharge of the water table by a run-off–runon system; ii) the water table under pressure below an impermeable layer; iii) tectonic activity and faults, with formation of artesian springs; iv) establishment of vegetation that colonize the area around a spring; v) entrapment of sand, with inputs from aeolian erosion; vi) formation of the spring mound, with stratified deposits of sand and secondary carbonates and sulphates (with no biogenic carbonate or sulphate accumulations); vii) paedogenesis of the sediments, with redoximorphic features and different carbonate accumulation; and viii) formation of a gypsic hardpan on top of the mound, by precipitation due to a saturated solution capillary rise with possible accumulation of aeolian gypsic sediments followed by meteoric induration of the gypsum.

Unfortunately, the time required for mounds to form remains unknown. Spring activity depended on the variation in rainfall during the Pleistocene and Holocene. In addition, the origins and proportions of sediments (i.e., allochthonous wind deposits vs. in situ inputs from spring discharge, as particles or precipitates) are difficult to define and measure.

### ACKNOWLEDGEMENTS

This project was supported by the French laboratory "Archéorient-Environnements et sociétés de l'Orient Ancien" (UMR 5133) and IRD (UMR IEES-Paris). We are grateful to Prof. Yann Callot for the introduction to and advice for this study, and to the Institute of Arid Regions of Medenine for facilities and field access, and in memory of its director, Houcine Khatteli. We thank Sandrine Caquineau (IRD, UMR LOCEAN) for the X-ray diffraction and electron microscope analyses and the ALYSES laboratory platform facility (IRD-SU) in Bondy, France. We thank the anonymous reviewers for their suggestions and Michael Corson for proofreading the English.

### CONFLICT OF INTEREST STATEMENT

The authors declare no conflict of interest.

### DATA AVAILABILITY STATEMENT

The data are available on request, and available in the dataverse files.

Raddadi A, Podwojewski, P. 2022. Location and morphological status of spring mounds in the Nefzaoua Province in western Tunisia in 2020. DataSuds, V1. https://doi.org/10.23708/U9GR0C.

Raddadi A, Podwojewski P. 2022. Sedimentary analysis of two spring mounds in the Nefzaoua Province in western Tunisia in 2020.", https://doi.org/10.23708/C1H9WJ, DataSuds, V1.

### ORCID

*Pascal Podwojewski* https://orcid.org/0000-0002-0812-5751

### REFERENCES

Aboukila, E. & Abdelaty, E. (2017) Assessment of saturated soil paste salinity from 1: 2.5 and 1: 5 soil-water extracts for coarse textured soils. *Alexandria Science Exchange Journal*, 38 (October–December, 722–732. Available from: https://doi.org/10.21608/asejaiqjsae.2017.4181

Adelsberger, K.A. & Smith, J.R. (2010) Paleolandscape and paleoenvironmental interpretation of spring-deposited sediments in Dakhleh Oasis, Western Desert of Egypt. *Catena*, 83(1), 7–22. Available from: https://doi.org/10.1016/j.catena.2010.06.009

Alonso-Zarza, A.M. (2003) Palaeoenvironmental significance of palustrine carbonates and calcretes in the geological record. *Earth-Science Reviews*, 60(3–4), 261–298. Available from: https://doi.org/10.1016/S0012-8252(02)00106-X

Alonso-Zarza, A.M. & Wright, V.P. (2010) Calcretes. *Developments in Sedimentology*, 61, 225–267. Available from: https://doi.org/10.1016/S0070-4571(09)06105-6

Barbieri, R., Stivaletta, N., Marinangeli, L. & Ori, G.G. (2006) Microbial signatures in sabkha evaporite deposits of Chott el Gharsa (Tunisia) and their astrobiological implications. *Planetary and Space Science*, 54(8), 726–736. Available from: https://doi.org/10.1016/j.pss.2006.04.003

Bendali, F., Floret, C., Le Floc'h, E. & Pontanier, R. (1990) The dynamics of vegetation and sand mobility in arid regions of Tunisia. *Journal of Arid Environments*, 18(1), 21–32. Available from: https://doi.org/10.1016/S0140-1963(18)30866-8

Besançon, J., Geyer, B., Muhesen, S. & Rousset, M.O. (2000) Les plateformes gypseuses et les tertres de source de la région de Ayn al Zarqa (Syrie du Nord) (Gypseous platforms and spring mounds near 'Ayn al Zarqa [North Syria]). In: *Bulletin de l'Association de géographes français, 77e année, 2000-1 (mars). L'eau dans les milieux arides et semi-arides*. Paris, France: La mondialisation de la distribution, pp. 10–16. Available from: https://doi.org/10.3406/bagf.2000.2142

Blinn, D.W., Hevly, R.H. & Davis, O.K. (1994) Continuous Holocene record of diatom stratigraphy, paleohydrology, and anthropogenic activity in a spring-mound in southwestern United States. *Quaternary Research*, 42(2), 197–205. Available from: https://doi.org/10.1006/qres.1994.1069

Bougeault, C., Vennin, E., Durlet, C., Muller, E., Mercuzot, M., Chavez, M., et al. (2019) Biotic–abiotic influences on modern Ca–Si-rich hydrothermal spring mounds of the Pastos Grandes Volcanic Caldera (Bolivia). *Minerals*, 9(6), 380. Available from: https://doi.org/10.3390/min9060380

Bravard, J.P., Mostafa, A., Garcier, R., Tallet, G., Ballet, P., Chevalier, Y., et al. (2016) Rise and fall of an Egyptian oasis: artesian flow, irrigation soils, and historical agricultural development in El deir, Kharga Depression, western desert of Egypt. *Geoarchaeology*, 31(6), 467–486. Available from: https://doi.org/10.1002/gea.21566

Brookes, I.A. (1993) Geomorphology and Quaternary geology of the Dakhla Oasis region, Egypt. *Quaternary Science Reviews*, 12(7), 529–552. Available from: https://doi.org/10.1016/0277-3791(93)90068-W

Bureau, P., & Roederer, P. (1960) *Contribution à l'étude des sols gypseux du Sud tunisien: croûtes et encroûtements gypseux de la partie sud du golfe de Gabès*. Tunis, Tunisie: Secretariat d'Etat à l'Agriculture, H.A.R., Section spéciale d'Etudes de Pédologie et d'Hydrologie, E-S 33, p. 41. Available from: https://www.documentation.ird.fr/hor/fdi:10976

Chepil, W.S. (1951a) Properties of soil which influence wind erosion: III. Effect of apparent density on erodibility. *Soil Science*, 71(2), 141–154. Available from: https://doi.org/10.1097/00010694-195102000-00008

Chepil, W.S. (1951b) Properties of soil which influence wind erosion: IV. State of dry aggregate structure. *Soil Science*, 72(5), 387–402. Available from: https://doi.org/10.1097/00010694-195111000-00007

Clarke, J., Bourke, M., Nelson, P., Manga, M. & Fonseca, J. (2007) The Dalhousie Mound Spring Complex as a Guide to Martian Landforms, Processes, and Exploration. In: *Proceedings of the 7th Australian Mars Exploration Conference*, Vol. 14. Clifton Hill, Vic: Mars Society Australia.

Coque, R. (1962) *La Tunisie présaharienne. Étude géomorphologique*. Paris: Colin.

Dixon, J.B. & Weed, S.B. (1989) *In minerals in soil environments*, 2nd edition, Book series n°1. Madison, WI: Soil Science Society of America.

Djoughi, Z. & Semra, A. (2017) *Contribution à l'étude du paléoenvironnement dans la région de Touggourt: Apport de la paléopédologie*. Master's thesis,. Ouargla, Algeria: Université Kasdi Merbah.

Drake, N.A. (1997) Recent aeolian origin of surficial gypsum crusts in southern Tunisia: geomorphological, archaeological and remote sensing evidence. *Earth Surface Processes and Landforms: the Journal of the British Geomorphological Group*, 22(7), 641–656. Available from: https://doi.org/10.1002/(SICI)1096-9837(199707)22:7<641::AID-ESP737>3.0.CO;2-R

Drake, N.A., Bryant, R.G., Millington, A.C. & Townshend, J.R. (1994) Playa sedimentology and geomorphology: mixture modelling applied to Landsat thematic mapper data of Chott el Djerid, Tunisia. In: Renault, R. & Last, W.L. (Eds.) *The sedimentology and geochemistry of Modern and Ancient Salt Lakes*. Society of Economic Mineralogists and Paleontologists, SEPM, Special Publication 50. Tulsa, Oklahoma: Society for Sedimentary Geology, pp. 3–12.

Drake, N.A., Eckardt, F.D. & White, K.H. (2004) Sources of sulphur in gypsiferous sediments and crusts and pathways of gypsum redistribution in southern Tunisia. *Earth Surface Processes and Landforms: the Journal of the British Geomorphological Research Group*, 29(12), 1459–1471. Available from: https://doi.org/10.1002/esp.1133

Essefi, E., Komatsu, G., Fairén, A.G., Chan, M.A. & Yaich, C. (2014) Models of formation and activity of spring mounds in the Mechertate-Chrita-Sidi El Hani System, Eastern Tunisia: implications for the habitability of Mars. *Lifestyles*, 4(3), 386–432. Available from: https://doi.org/10.3390/life4030386

Fontes, J.C. & Pouchan, P. (1975) Concretions of Abbe Lake (Djibouti). Hydroclimatic recorders of Hologene. *Comptes Rendus à l'Académie des Sciences, série D*, 280(4), 383–386.

Franchi, F. & Frisia, S. (2020) Crystallization pathways in the Great Artesian Basin (Australia) spring mound carbonates: implications for life signatures on earth and beyond. *Sedimentology*, 67(5), 2561–2595. Available from: https://doi.org/10.1111/sed.12711

Gonçalvès, J., Petersen, J., Deschamps, P., Hamelin, B. & Baba, S.O. (2013) Quantifying the modern recharge of the "fossil" Sahara aquifers. *Geophysical Research Letters*, 40(11), 2673–2678. Available from: https://doi.org/10.1002/grl.50478, 2013.

Guo, Z., Petit-Maire, N. & Kröpelin, S. (2000) Holocene non-orbital climatic events in present-day arid areas of northern Africa and China. *Global and Planetary Change*, 26(1–3), 97–103. Available from: https://doi.org/10.1016/S0921-8181(00)00037-0

Hadj Ammar, F., Chkir, N., Zouari, K., Hamelin, B., Deschamps, P. & Aigoun, A. (2014) Hydro-geochemical processes in the complexe terminal aquifer of southern Tunisia: an integrated investigation based on geochemical and multivariate statistical methods. *Journal of African Earth Sciences*, 100, 81–95. Available from: https://doi.org/10.1016/j.jafrearsci.2014.06.015

Haj-Amor, Z., Tóth, T., Ibrahimi, M.K. & Bouri, S. (2017) Effects of excessive irrigation of date palm on soil salinization, shallow groundwater properties, and water use in a Saharan oasis. *Environmental Earth Sciences*, 76(17), 1–13, 590. Available from: https://doi.org/10.1007/s12665-017-6935-8

Harris, C. (1981) Oases in the desert: the mound springs of northern south Australia. *Proceedings of the Royal Geographical Society Australasia (SA Branch)*, 81, 26–39.

Idris, H. (1996) Springs in Egypt. *Environmental Geology*, 27(2), 99–104. Available from: https://doi.org/10.1007/BF01061678

IUSS Working Group WRB. (2022) *World reference base for soil resources. International soil classification system for naming soils and creating legends for soil maps*. 4th edition, Vienna, Austria: International Union of Soil Sciences (IUSS).

Jones, A. & Millington, A. (1986) Spring mound and aioun mapping from Landsat TM imagery in south-central Tunisia. *Remote sensing for resources development and environmental management. International symposium*, 7. Rotterdam, Boston MA: A. A Balkema, pp. 607–613.

Jouquet, P., Henry-des-Tureaux, T., Bouet, C., Labiadh, M., Caquineau, S., Aroui Boukbida, H., et al. (2021) Bioturbation and soil resistance to wind erosion in Southern Tunisia. *Geoderma*, 403, 115198. Available from: https://doi.org/10.1016/j.geoderma.2021.115198

Keppel, M.N., Clarke, J.D., Halihan, T., Love, A.J. & Werner, A.D. (2011) Mound springs in the arid Lake Eyre South region of South Australia: a new depositional tufa model and its controls. *Sedimentary Geology*, 240(3–4), 55–70. Available from: https://doi.org/10.1016/j.sedgeo.2011.08.001

Khatelli, H. & Gabriels, D. (2000) Effect of wind direction on aeolian sand transport in southern Tunisia. *International Agrophysics*, 14(3), 291–296.

Kraiem, Z., Zouari, K., Chkir, N. & Agoune, A. (2014) Geochemical characteristics of arid shallow aquifers in Chott Djerid, South-Western Tunisia. *Journal of Hydro-Environment Research*, 8(4), 460–473. Available from: https://doi.org/10.1016/j.jher.2013.06.002

Lasram, M. (1990) Les systèmes agricoles oasiens dans le Sud de la Tunisie. In: Dollé, V. & Toutain, G. (Eds.) *Les systèmes agricoles oasiens. Montpellier: CIHEAM*, (Options Méditerranéennes: Série A. Séminaires Méditerranéens, n. 11). Paris: CIHEAM, pp. 21–27.

Le Houerou, H.N. (1959) Recherches écologiques et floristiques sur la végétation de la Tunisie Méridionale. Mémoire de l'Institut de recherches sahariennes. Université d'Alger.

Li, Y., Zhang, C., Chen, C. & Chen, H. (2018) Calculation of capillary rise height of soils by SWCC model. *Hindawi, Advances in Civil Engineering*, 218, 5190354. Available from: https://doi.org/10.1155/2018/5190354

Lu, N. & Likos, W.J. (2004) Rate of capillary rise in soil. *Journal of Geotechnical and Geoenvironmental Engineering*, 130(6), 646–650. Available from: https://doi.org/10.1061/(ASCE)1090-0241(2004)130:6(646)

Marlet, S., Bouksila, F. & Bahri, A. (2009) Water and salt balance at irrigation scheme scale: a comprehensive approach for salinity assessment in a Saharan oasis. *Agricultural Water Management*, 96(9), 1311–1322. Available from: https://doi.org/10.1016/j.agwat.2009.04.016

McCarthy, T.S., Ellery, W.N., Backwell, L., Marren, P., De Klerk, B., Tooth, S., et al. (2010) The character, origin and palaeoenvironmental significance of the Wonderkrater spring mound, South Africa. *Journal of African Earth Sciences*, 58(1), 115–126. Available from: https://doi.org/10.1016/j.jafrearsci.2010.02.004

Monaco, A., Belhouchet, L., Brahim, H.B.H., Fraj, T.B., Nasr, J.B., Boussoffara, R., et al. (2020) Megalithic structures of the northern sahara (chott el Jerid, Tunisia). *Cartagine. Studi e Ricerche*, 5, 1–2. Available from: https://doi.org/10.13125/caster/4078

Neal, J.T. & Motts, W.S. (1967) Recent geomorphic changes in playas of western United States. *The Journal of Geology*, 75(5), 511–525. Available from: https://doi.org/10.1086/627279

Niftah, S., Debénath, A. & Miskovsky, J.C. (2005) Origine du remplissage sédimentaire des grottes de Témara (Maroc) d'après l'étude des minéraux lourds et l'étude exoscopique des grains de quartz. *Quaternaire. Revue de l'Association française Pour l'étude du Quaternaire*, 16(2), 73–83. Available from: https://doi.org/10.4000/quaternaire.295

Ori, G.G. (2010) The sedimentary record of modern and ancient dry lakes. In: Cabrol, N.A. & Grin, E.A. (Eds.) *Lakes on Mars*. Amsterdam: Elsevier, pp. 307–322. Available from: https://doi.org/10.1016/B978-0-444-52854-4.00011-8

OSS. (2003) *Système Aquifère du Sahara Septentrional: Hydrogéologie, volume II. Observatoire du Sahara et du Sahel*. Tunis: Observatoire du Sahara et du Sahel, p. 130. Available from: http://www.oss-online.org/sites/default/files/publications/OSS-SASSHYDROGEOLOGIE-II.pdf

Pansu, M. & Gautheyrou, J. (2006) *Handbook of soil analysis. Mineralogical, organic and inorganic methods*. Berlin, Heidelberg, New York: Springer.

Pellicer, X.M., Linares, R., Gutiérrez, F., Comas, X., Roqué, C., Carbonel, D., et al. (2014) Morpho-stratigraphic characterization of a tufa mound complex in the Spanish Pyrenees using ground penetrating radar and trenching, implications for studies in Mars. *Earth and Planetary Science Letters*, 388, 197–210. Available from: https://doi.org/10.1016/j.epsl.2013.11.052

Ponder, W.F. (1986) Mound springs of the great artesian basin. In: *Limnology in Australia*. Dordrecht: Springer, pp. 403–420. Available from: https://doi.org/10.1007/978-94-009-4820-4_25

Pouget, M. (1968) Contribution à l'étude des croûtes et encroûtements gypseux de nappe dans le sud tunisien. *Cahiers ORSTOM série pédologie*, 6, 309–365.

Powell, O. & Fensham, R. (2015) The history and fate of the Nubian sandstone aquifer springs in the oasis depressions of the Western Desert, Egypt. *Hydrogeology Journal*, 24(2), 395–406. Available from: https://doi.org/10.1007/s10040-015-1335-1

Powell, O., Silcock, J. & Fensham, R. (2015) Oases to oblivion: the rapid demise of springs in the south-eastern Great Artesian Basin, Australia. *Groundwater*, 53(1), 171–178. Available from: http://citeseerx.ist.psu.edu/viewdoc/download?doi=10.1.1.834.3475&rep=rep1&type=pdf, https://doi.org/10.1111/gwat.12147

Raddadi, A. (2021) *Les paysages du Nefzaoua, une interaction entre l'eau, le vent et les hommes*. Ph.D. thesis. Lyon: Université Lumière Lyon 2, Ecole doctorale des sciences sociales, UFR Temps et territoires, Département de géographie. Available from: https://drive.google.com/file/d/1rtMsMtqAVW7NWYlBXgwRtDd9jSssly-3/view

Raddadi, A., Callot, Y. & Podwojewski, P. (2021) Un patrimoine en péril: les tertres du Nefzaoua dans le sud tunisien. In: Reynard, E. & Bussard, J. (Eds.) *Géopatrimoines et territoires. Geo-Regards*, Neuchatel, Switzerland: Institut de géographie de l'Université de Neuchâtel, Éditions Alphil-Presses universitaires suisses, 14, pp. 95–118. Available from: https://doi.org/10.33055/Geo-Regards.2021.014.01

Raddadi, A. & Podwojewski, P. (2022a) Spring mounds of the Nefzaoua oases in Tunisia: irreversible degradation of exceptional geomorphic structures. *Journal of Arid Environments*, 205, 104806. Available from: https://doi.org/10.1016/j.jaridenv.2022.104806

Raddadi, A. & Podwojewski, P. (2022b) *Location and morphological status of spring mounds in the Nefzaoua Province in western Tunisia in 2020*, Vol. V1. DataSuds. Available from: https://doi.org/10.23708/U9GR0C

Raddadi, A. & Podwojewski, P. (2022c) *Sedimentary analysis of two spring mounds in the Nefzaoua Province in western Tunisia in 2020*, Vol. V1. DataSuds. Available from: https://doi.org/10.23708/C1H9WJ

Roberts, C.R. & Mitchell, C.W. (1987) Spring mounds in southern Tunisia. *Geological Society, London, Special Publications*, 35(1), 321–334. Available from: https://doi.org/10.1144/GSL.SP.1987.035.01.22

Scholl, D.W. (1960) Pleistocene algal pinnacles at Searles Lake, California. *Journal of Sedimentary Research*, 30(3), 414–431.

Scholl, D.W. & Taft, W.H. (1964) Algae, contributors to the formation of calcareous tufa, mono lake, California. *Journal of Sedimentary Research*, 34(2), 309–319. Available from: https://doi.org/10.1306/74D71041-2B21-11D7-8648000102C1865D

Schulz, E., Abichou, A., Hachicha, T., Pomel, S., Salzmann, U. & Zouari, K. (2002) Sebkhas as ecological archives and the vegetation and landscape history of southeastern Tunisia during the last two millennia. *Journal of African Earth Sciences*, 34(3–4), 223–229. Available from: https://doi.org/10.1016/S0899-5362(02)00021-0

Sghaier, M. (1999) *Les oasis de la Région de Nefzaoua. Interaction between migration, Land & Water Management and resource exploitation in the oases of the Maghreb, IMAROM*, Working paper series 3. The Netherlands: Univ. of Amsterdam, p. 37.

Stivaletta, N. & Barbieri, R. (2009) Endolithic microorganisms from spring mound evaporite deposits (southern Tunisia). *Journal of Arid Environments*, 73(1), 33–39. Available from: https://doi.org/10.1016/j.jaridenv.2008.09.024

Swezey, C.S. (1996) Structural controls on Quaternary depocentres within the Chotts Trough region of southern Tunisia. *Journal of African Earth Sciences*, 22(3), 335–347. Available from: https://doi.org/10.1016/0899-5362(96)00012-7

Swezey, C.S. (2003) The role of climate in the creation and destruction of continental stratigraphic records: an example from the northern margin of the Sahara Desert. In: *SEPM (Society for Sedimentary Geology), Special Publication* No. 77. Tulsa, Oklahoma: SEPM, Society for Sedimentary Geology, pp. 207–225.

Torab, M. (2014) Geomorphology of fossil springs mounds in some selected portions of western desert oasis of Egypt. In: Efe, R. & Ozturk, M. (Eds.) *Environment and ecology in the Mediterranean region II*, Vol. 27. Cambridge Scholars Publishing, Chapter 27, pp. 317–329.

Torab, M. (2021) Geomorphology of fossil springs mounds near el Gedida village, Dakhla oasis, western desert of Egypt. *The Egyptian Journal of Environment Change*, 13(1), 23–32. Available from: https://doi.org/10.21608/ejec.2021.149015

Trichet, J. (1963) Description d'une forme d'accumulation de gypse par voie éolienne dans le Sud tunisien. *Bulletin de la Société Géologique de France*, 7(4), 617–621. Available from: https://doi.org/10.2113/gssgfbull.S7-V.4.617

Trousset, P. (1986) Les oasis présahariennes dans l'Antiquité: partage de l'eau et division du temps. *Antiquités Africaines*, 22(1), 163–193. Available from: https://doi.org/10.3406/antaf.1986.1130

Vieillefon, J. (1979) Contribution à l'amélioration de l'étude analytique des sols gypseux. *Cahiers ORSTOM, série Pédologie*, XVII(3), 195–223.

Walkley, A. (1947) A critical examination of a rapid method for determining organic carbon in soils effect of variations in digestion conditions and of inorganic soil constituents. *Soil Science*, 63(4), 251–264. Available from: https://doi.org/10.1097/00010694-194704000-00001

Watson, A. (1985) Structure, chemistry and origins of gypsum crusts in southern Tunisia and the central Namib Desert. *Sedimentology*, 32(6), 855–875. Available from: https://doi.org/10.1111/j.1365-3091.1985.tb00737.x

Watson, A. (1988) Desert gypsum crusts as palaeoenvironmental indicators: a micropetrographic study of crusts from southern Tunisia and the central Namib Desert. *Journal of Arid Environments*, 15(1), 19–42. Available from: https://doi.org/10.1016/S0140-1963(18)31002-4

Watts, S.H. (1973) Mound springs. *Australian Geographer*, 13, 52–53.

White, K. & Drake, N. (1993) Mapping the distribution and abundance of gypsum in south-central Tunisia from Landsat thematic mapper data. *Zeitschrift für Geomorphologie*, 37(3), 309–325. Available from: https://doi.org/10.1127/zfg/37/1993/309

Williams, A.F. & Holmes, J.W. (1978) A novel method of estimating the discharge of water from mound springs of the Great Artesian Basin, Central Australia. *Journal of Hydrology*, 38(3–4), 263–272. Available from: https://doi.org/10.1016/0022-1694(78)90073-2

Youcef, F. (2016) *Contribution à la reconstitution du paléoenvironnement au Sahara septentrional dans les sols de bassins endoréiques: Cas de la région de Ouargla*. Ph.D. dissertation,. Ouargla, Algeria: Université Kasdi Merbah.

Zammouri, M., Siegfried, T., El-Fahem, T., Kriâa, S. & Kinzelbach, W. (2007) Salinization of groundwater in the Nefzawa oases region, Tunisia: results of a regional-scale hydrogeologic approach. *Hydrogeology Journal*, 15(7), 1357–1375. Available from: https://doi.org/10.1007/s10040-007-0185-x

## SUPPORTING INFORMATION

Additional supporting information can be found online in the Supporting Information section at the end of this article.

**How to cite this article:** Raddadi, A. & Podwojewski, P. (2024) The internal structure of spring mounds of Nefzaoua oasis in Tunisia: Formation of an original geomorphic structure. *Earth Surface Processes and Landforms*, 49(2), 901–917. Available from: https://doi.org/10.1002/esp.5734

## Supporting information

| | |
|---|---|
| esp5734-sup-0001-FigureS1.pdf<br>PDF document, 374.2 KB | **Figure S1.** Sections A, B, C, D, Variation in texture; boundaries of units and strata. |
| esp5734-sup-0002-FigureS2_photo.pdf<br>PDF document, 879.6 KB | **Figure S2.** Photograph of section B, with boundaries between major units. |
| esp5734-sup-0003-FigureS3.pdf<br>PDF document, 90.6 KB | **Figure S3.** Section B. Variation in texture: cS: coarse Sand (2000-200 µm), fS: fine Sand (200-50 µm), C + Si: Clay+Silt (<50 µm), gypsum and carbonate contents (%), electrical conductivity (EC) (mS $cm^{-1}$), and soil organic carbon (SOC) (mg $kg^{-1}$). |
| esp5734-sup-0004-FigureS4_photo.pdf<br>PDF document, 256.6 KB | **Figure S4.** Photograph of section C, with boundaries between major units. |
| esp5734-sup-0005-FigureS5.pdf<br>PDF document, 87.3 KB | **Figure S5.** Section C. Variation in texture: cS: coarse Sand (2000-200 µm), fS: fine Sand (200-50 µm), C + Si: Clay+Silt (<50 µm), gypsum and carbonate contents (%), EC (mS $cm^{-1}$), and soil organic carbon (SOC) (mg $kg^{-1}$). |
| esp5734-sup-0006-FigureS6R.pdf<br>PDF document, 3.3 MB | **Figure S6.** BEAM photographs of aeolian deposits associated with microprobe determination of coatings (Mn, Fe, carbonates, gypsum and clay). |
| esp5734-sup-0007-FigureS7R.pdf<br>PDF document, 111.8 KB | **Figure S7.** X-ray diffraction of clay coatings of section C level C2 and section D level D6.<br>in black: oriented clays, blue: glycol treated, red: heated.<br>C: chlorite; I: illite; K: kaolinite; P: palygorskite; S: smectite. |
| esp5734-sup-0008-FigureS8R.pdf<br>PDF document, 712.7 KB | **Figure S8.** Detailed photographs from different sections: A and B) occurrence of gleyic and or stagnic pedological processes in the sediments; C) Iron And Manganese oxide accumulation; D) gypsum crust at the top of section D. |
| esp5734-sup-0009-TABLE_S1.docx<br>Word 2007 document , 205.7 KB | **Table S1.** Analytical results. |

**Figure S1.**
Sections A, B, C, D, Variation in texture; boundaries of units and strata

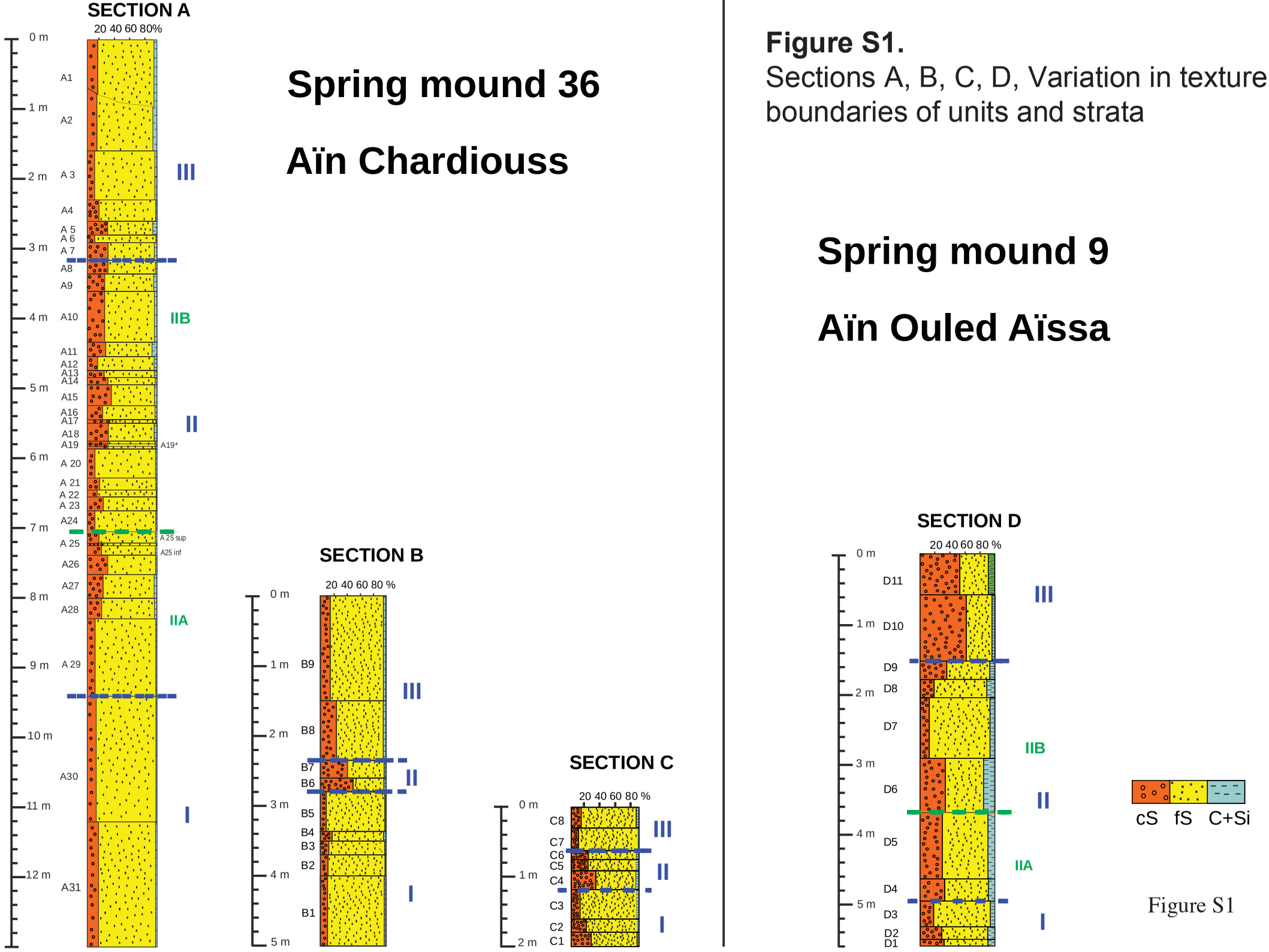


Figure S1


**Figure S2**
Photograph of section B, with boundaries between major units.

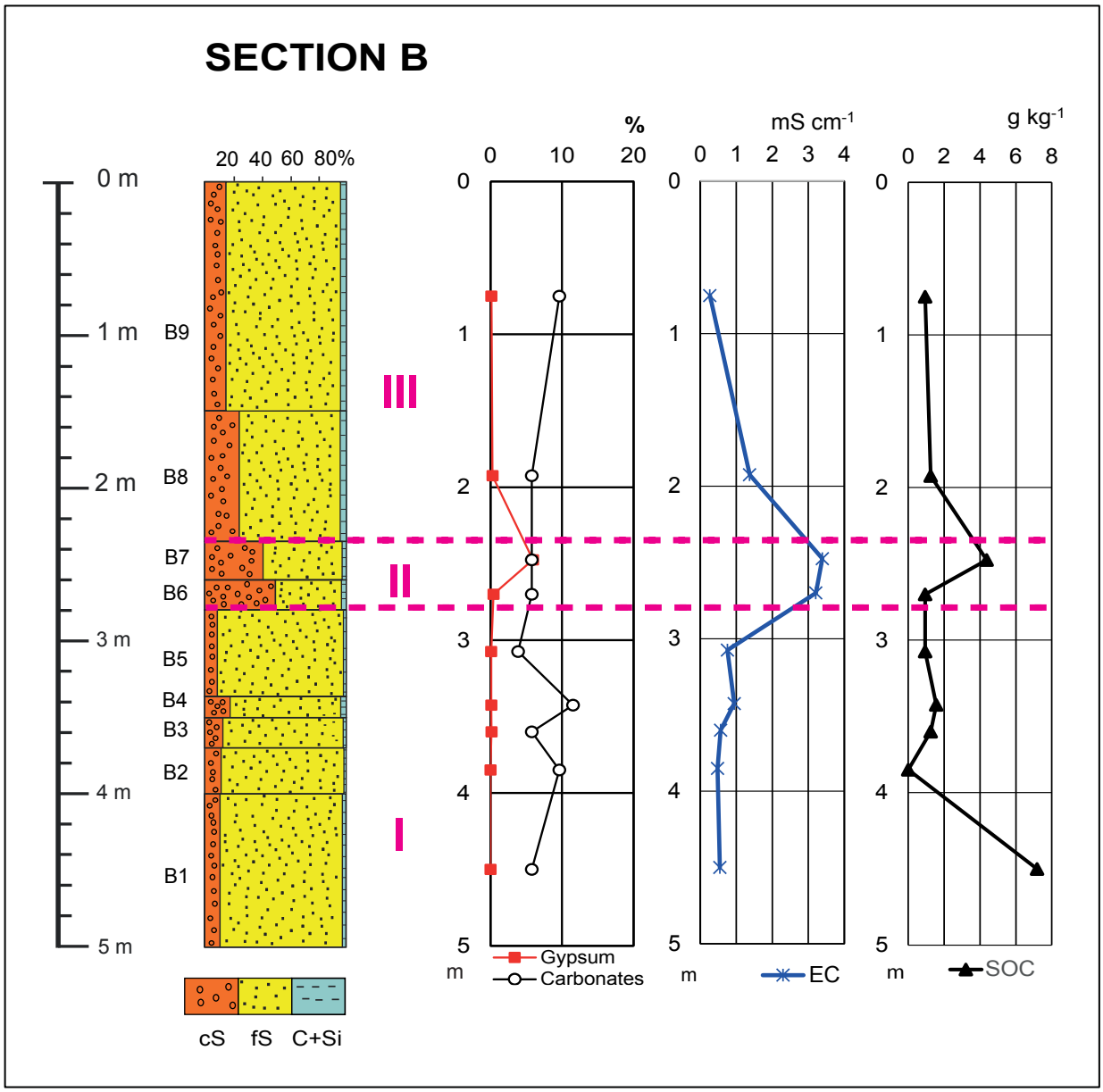


**Figure S3.**
Section B. Variation in texture: cS: coarse Sand (2000-200 µm), fS: fine Sand (200-50 µm), C+Si: Clay+Silt (<50 µm), gypsum and carbonate contents (%), electrical conductivity (EC) (mS $cm^{-1}$), and soil organic carbon (SOC) (mg $kg^{-1}$).

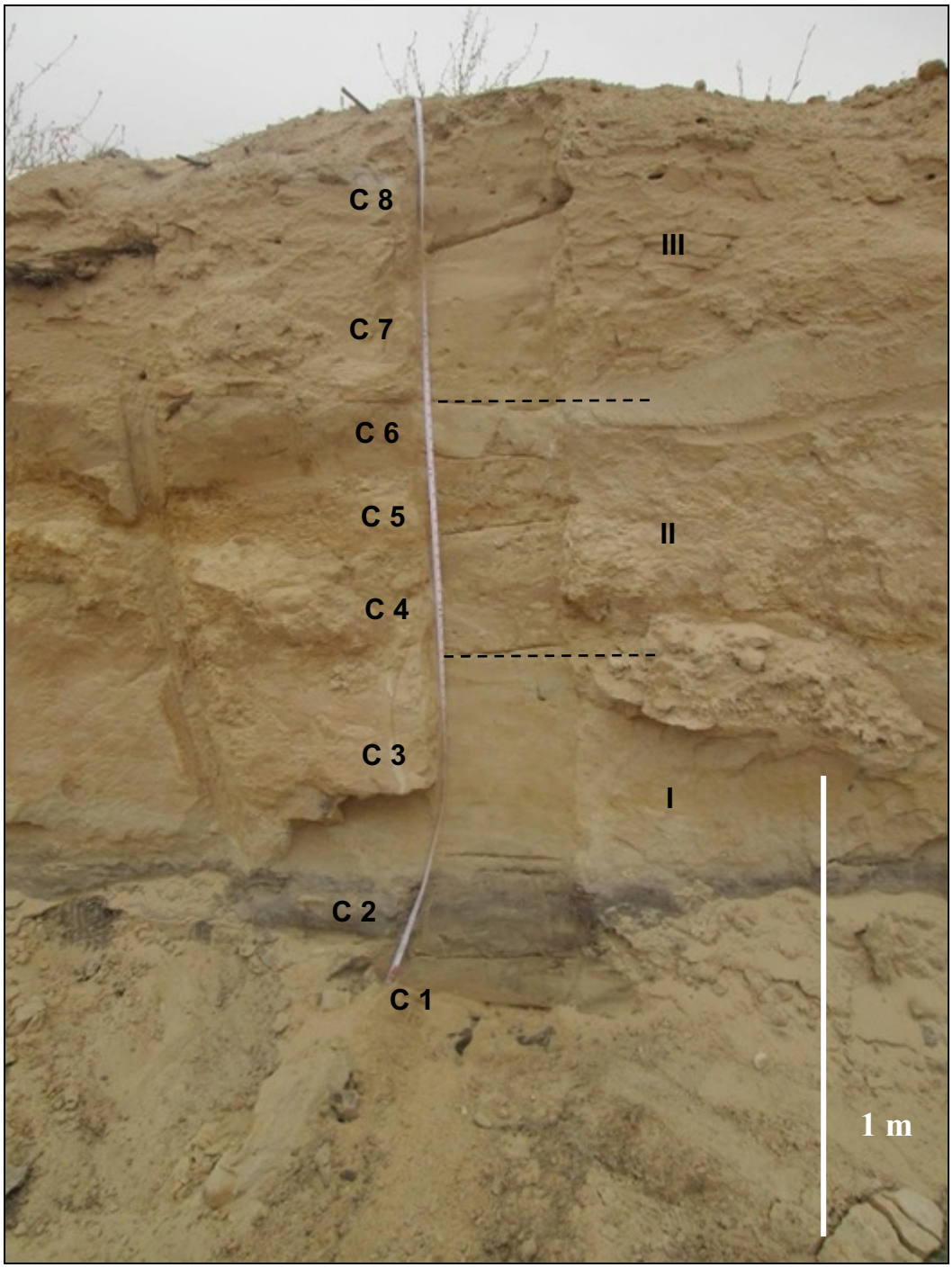


**Figure S4.**
Photograph of section C, with boundaries between major units.

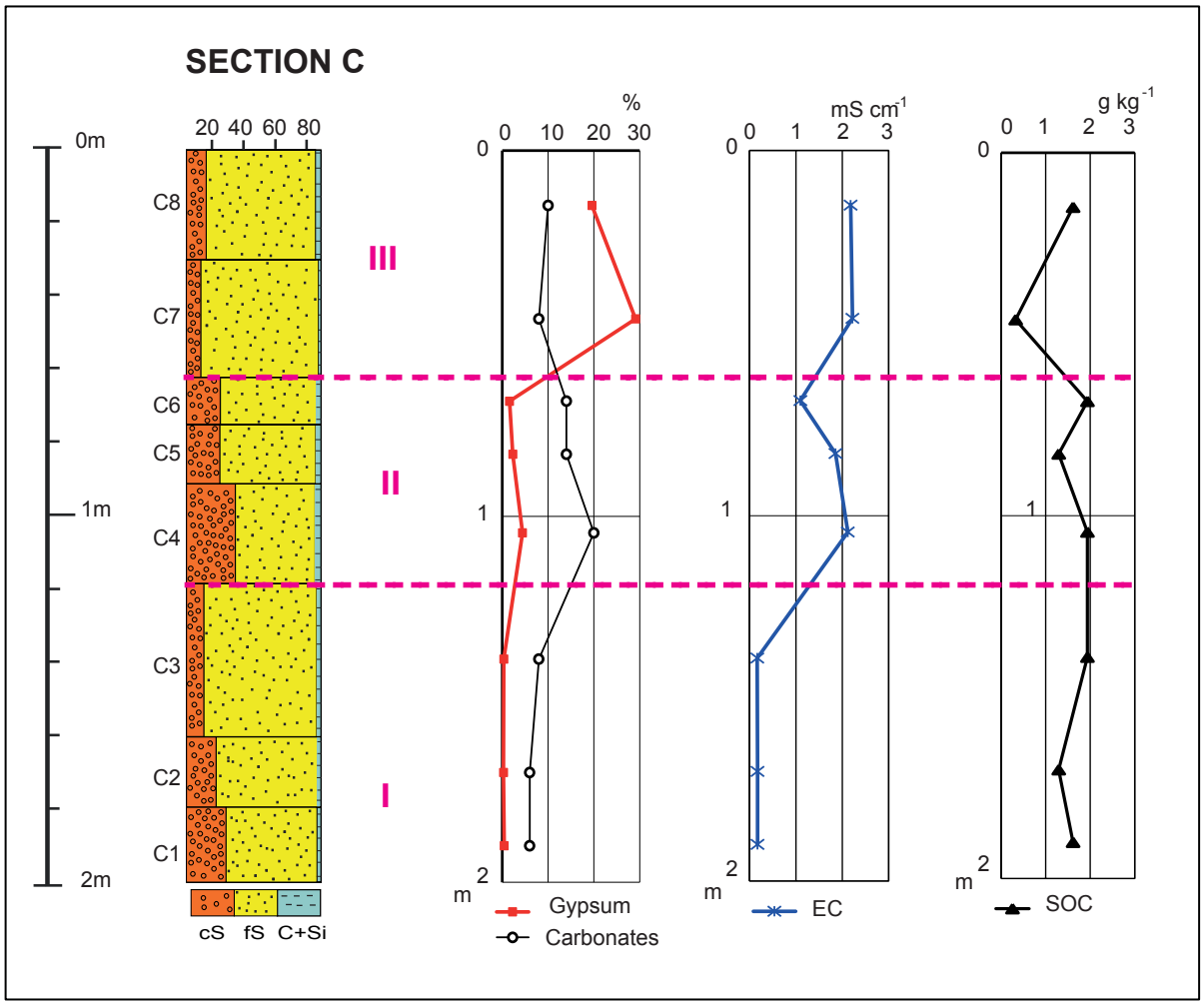


**Figure S5.**
Section C. Variation in texture: cS: coarse Sand (2000-200 µm), fS: fine Sand (200-50 µm), C+Si: Clay+Silt (<50 µm), gypsum and carbonate contents (%), EC (mS $cm^{-1}$), and soil organic carbon (SOC) (mg $kg^{-1}$).

**Figure S6.** BEAM photographs of aeolian deposits associated with microprobe determination of coatings (Mn, Fe, carbonates, gypsum and clay).

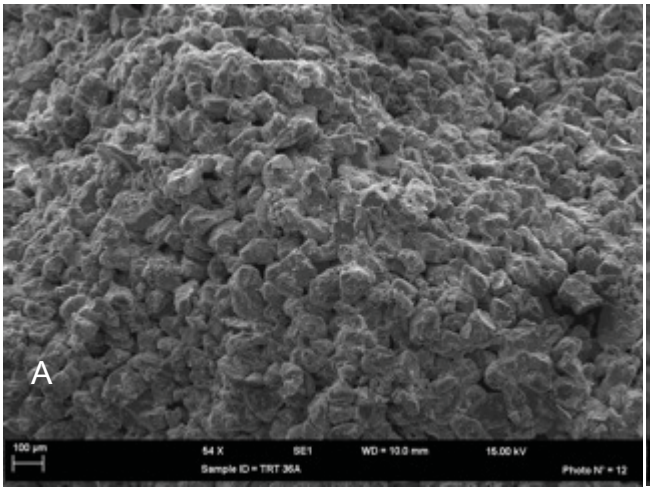


A) Homometric quartz grains; aeolian deposits

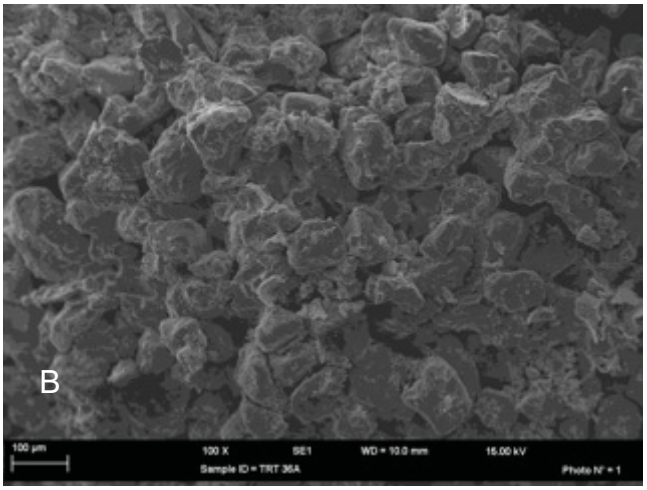


B) Homometric quartz grains; aeolian deposits

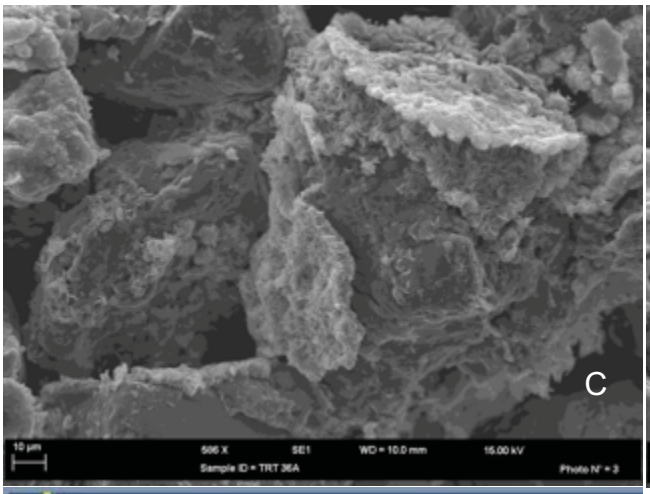


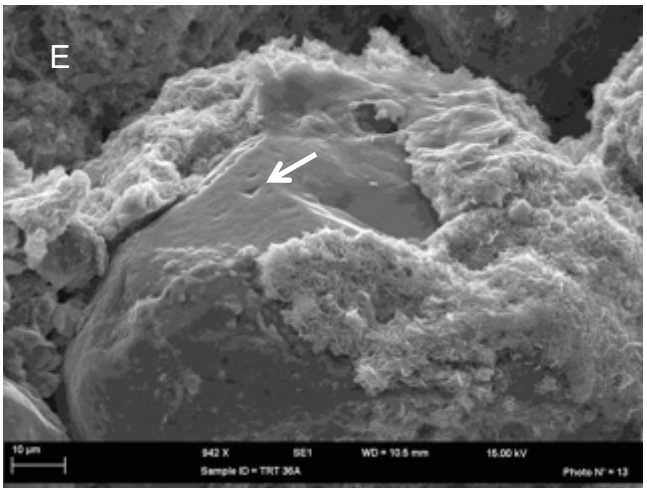


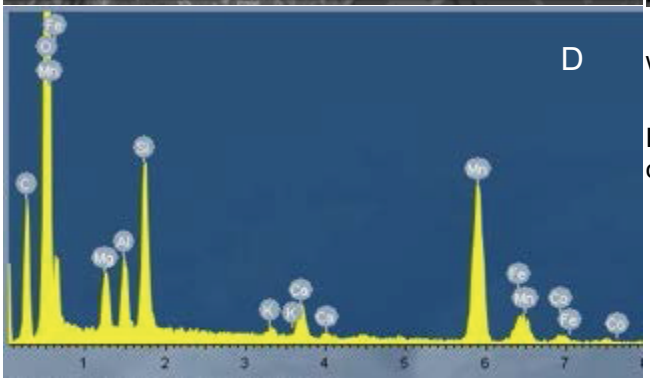


C) and D) Coatings of manganese oxides associated with fibrous clays (palygorskite) over a quartz grain.

E) Detail of quartz grain with coatings of manganese oxides and dissolution features (arrow).

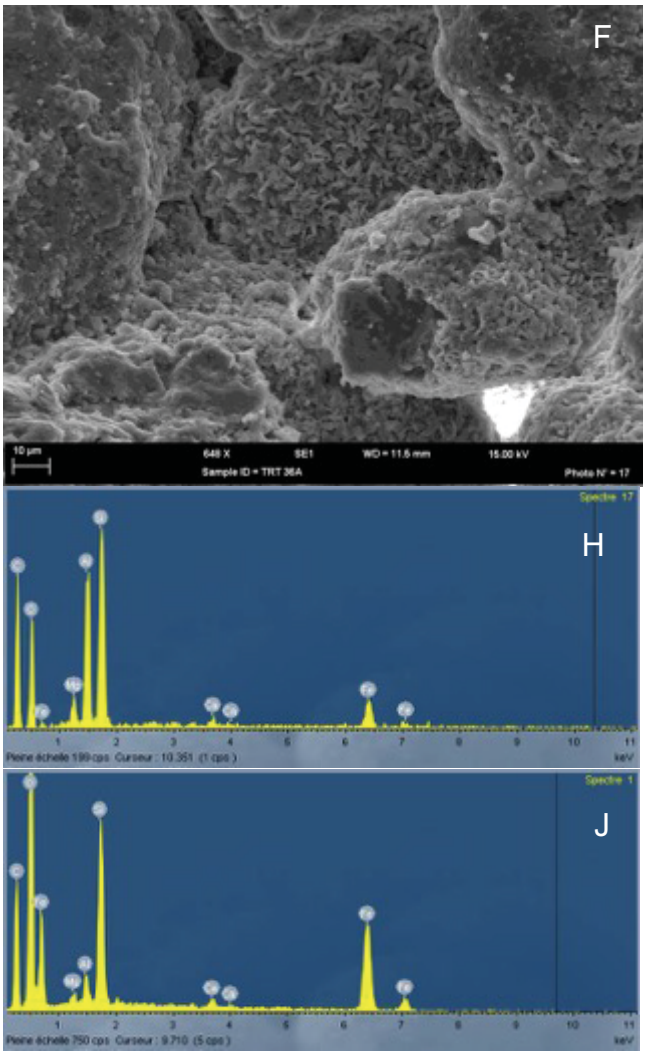


F), G) and H) kaolinite associated with coatings of iron oxides.

I) and J) coatings of iron oxides

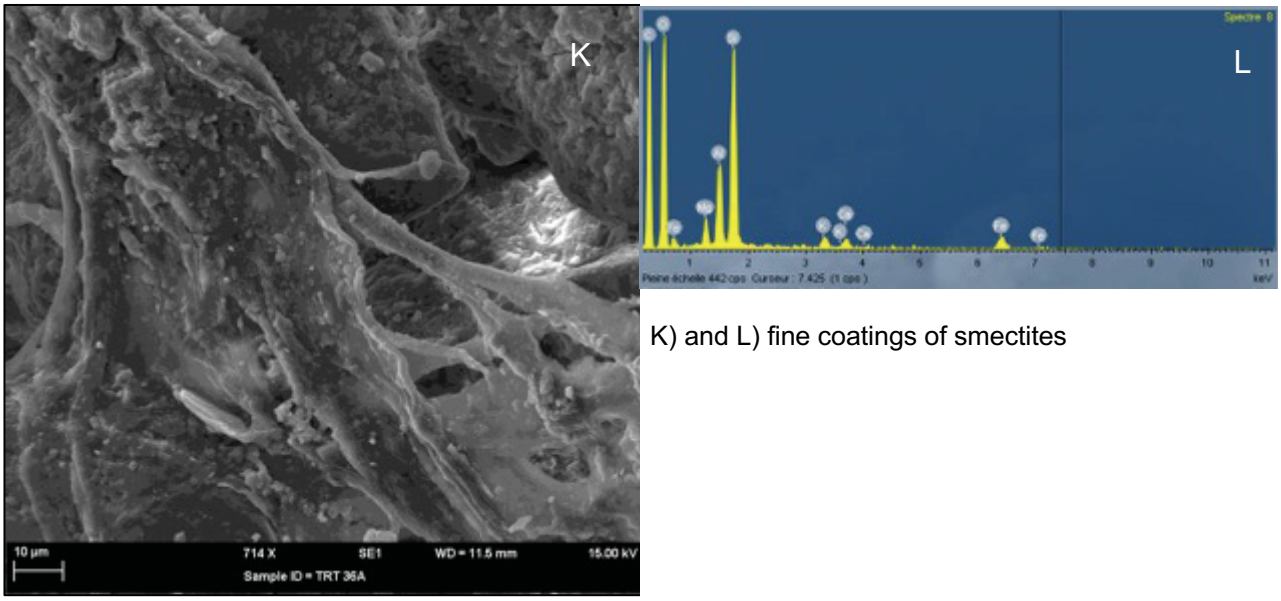


K) and L) fine coatings of smectites

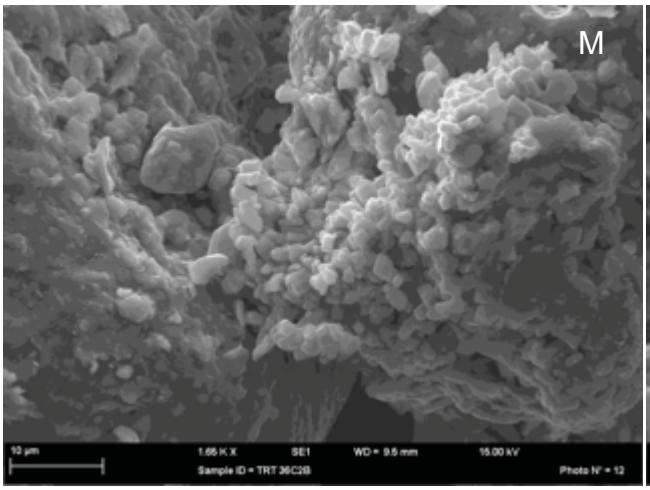


M) Micrometric crystals of calcite coating a quartz grain

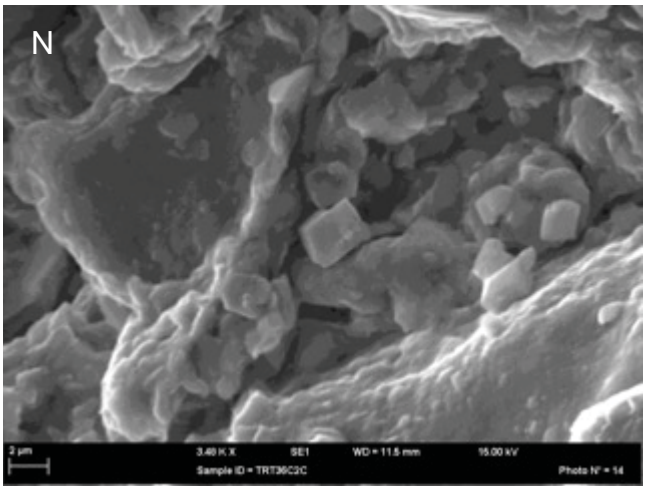


N) Detail of micrometric crystals of calcite coating a quartz grain

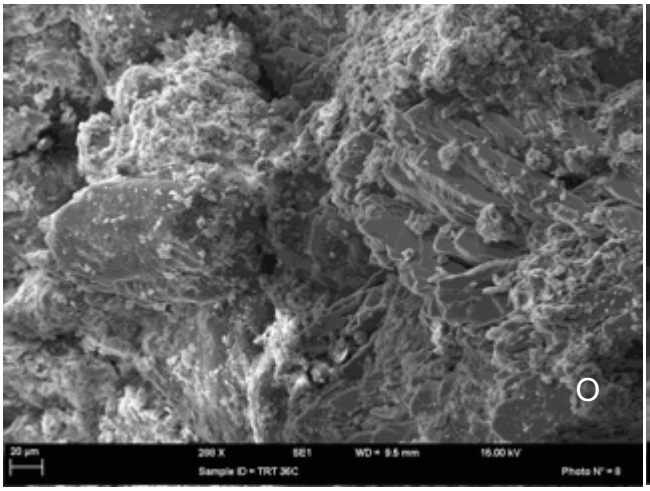


O) gypsum crystals 100µm long

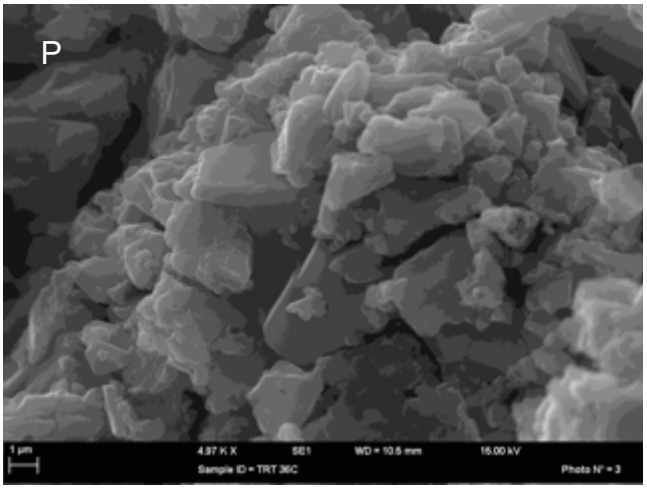


O) detail of micrometric gypsum crystals

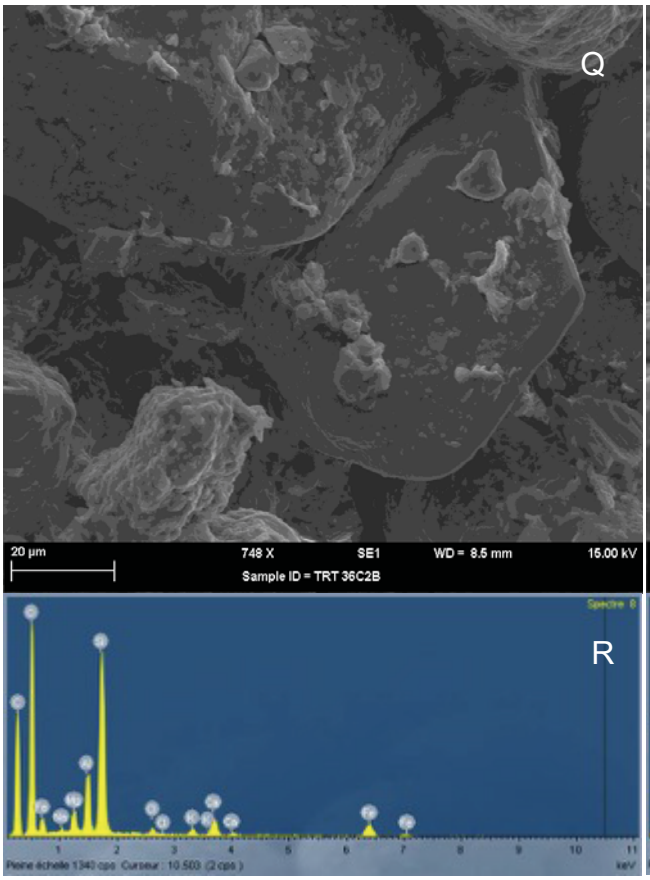


Q) and R) smectite coatings over a quartz grain

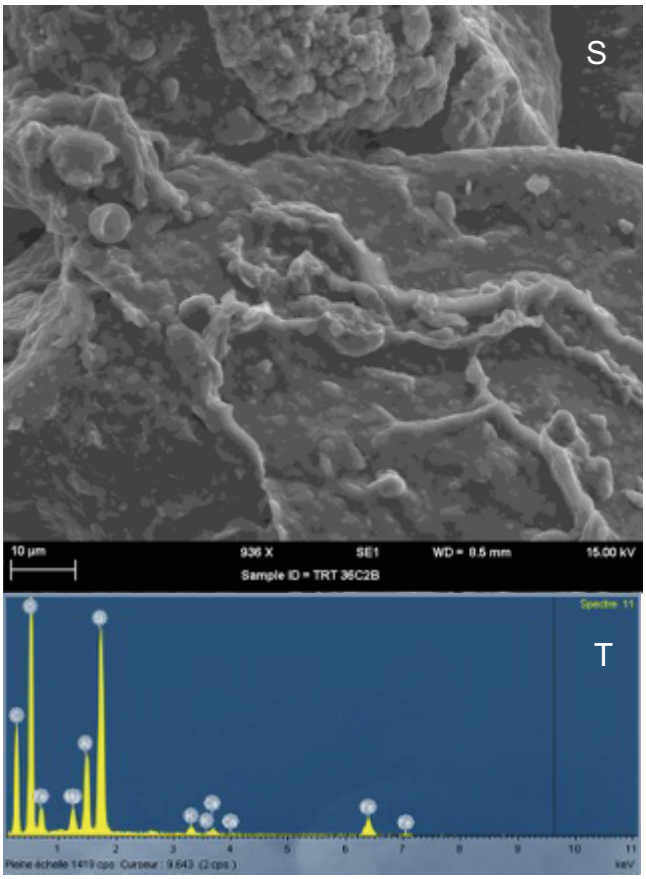


S) and T) smectite coatings in sheets over a quartz grain

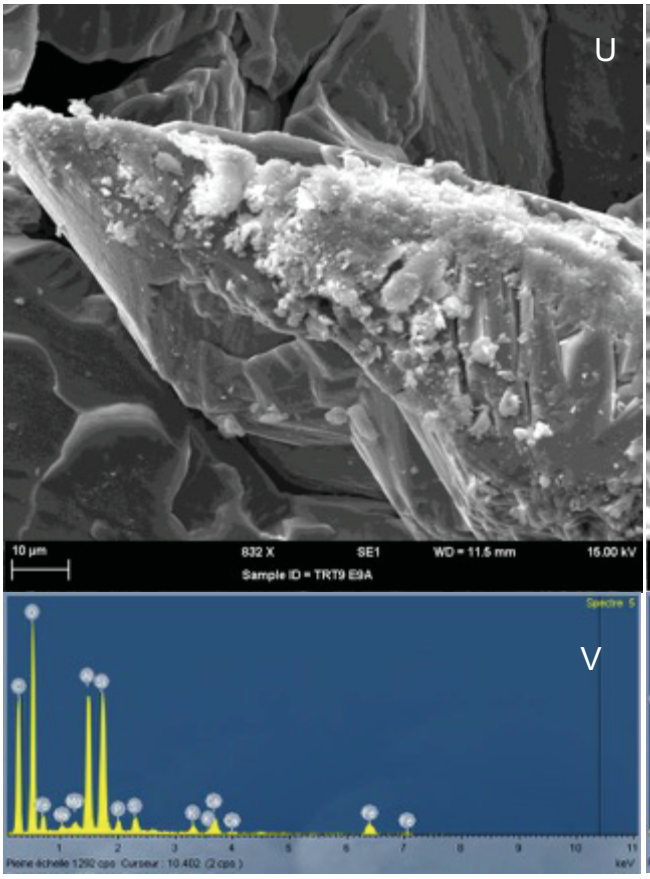


U) and V) coatings of kaolinite over gypsum crystal

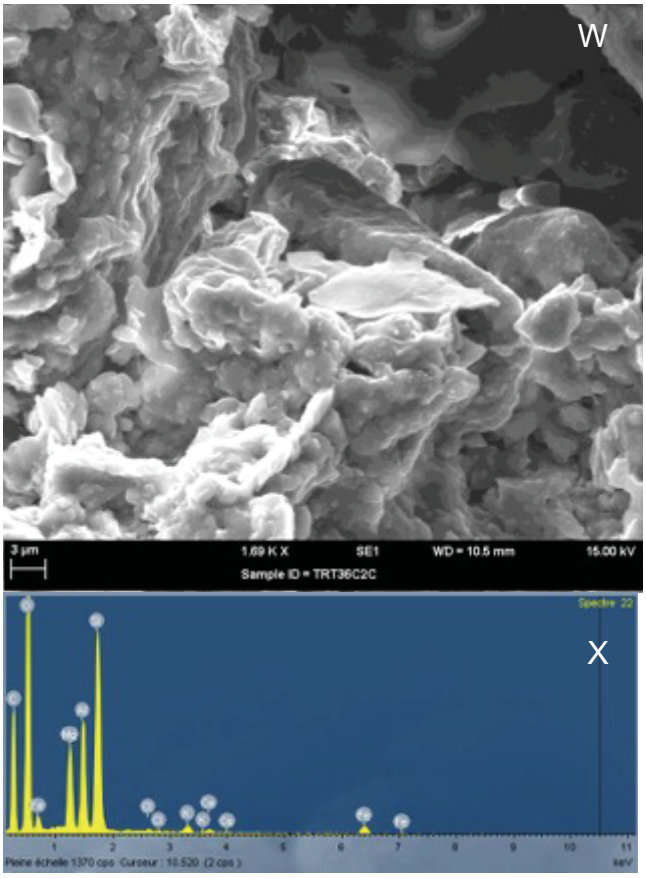


W) and X) Coatings of smectite and fibroux clays

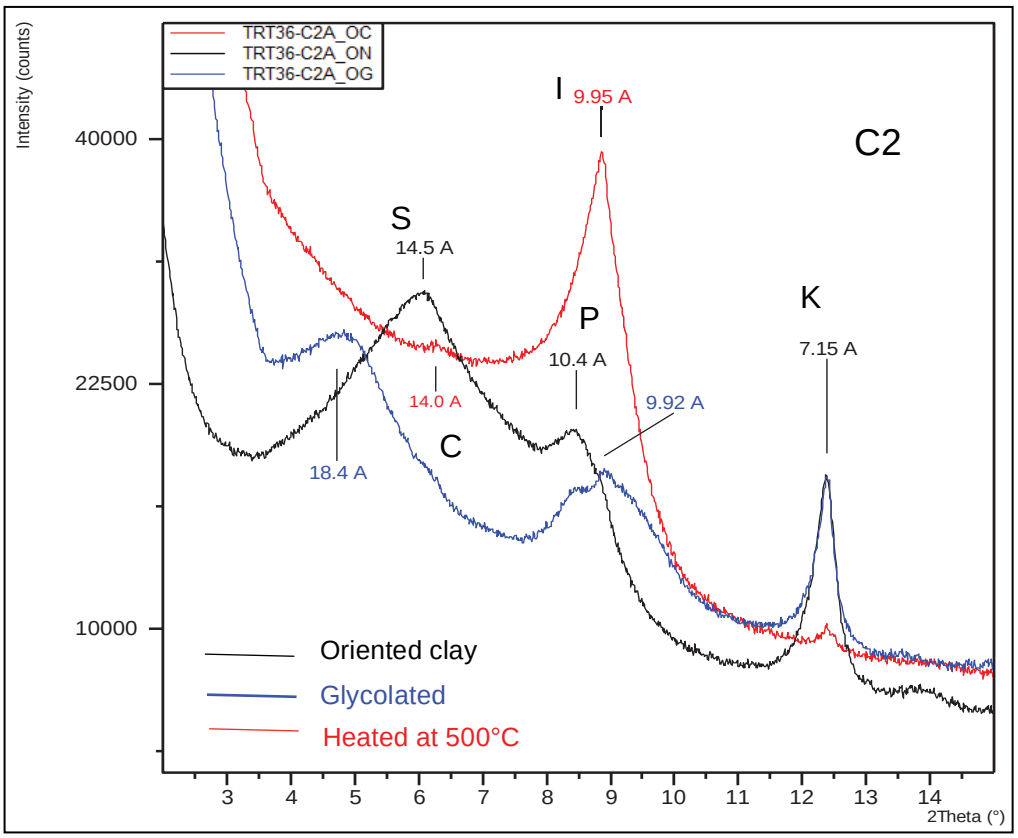


XRD of the C2 layer at the base of Section C

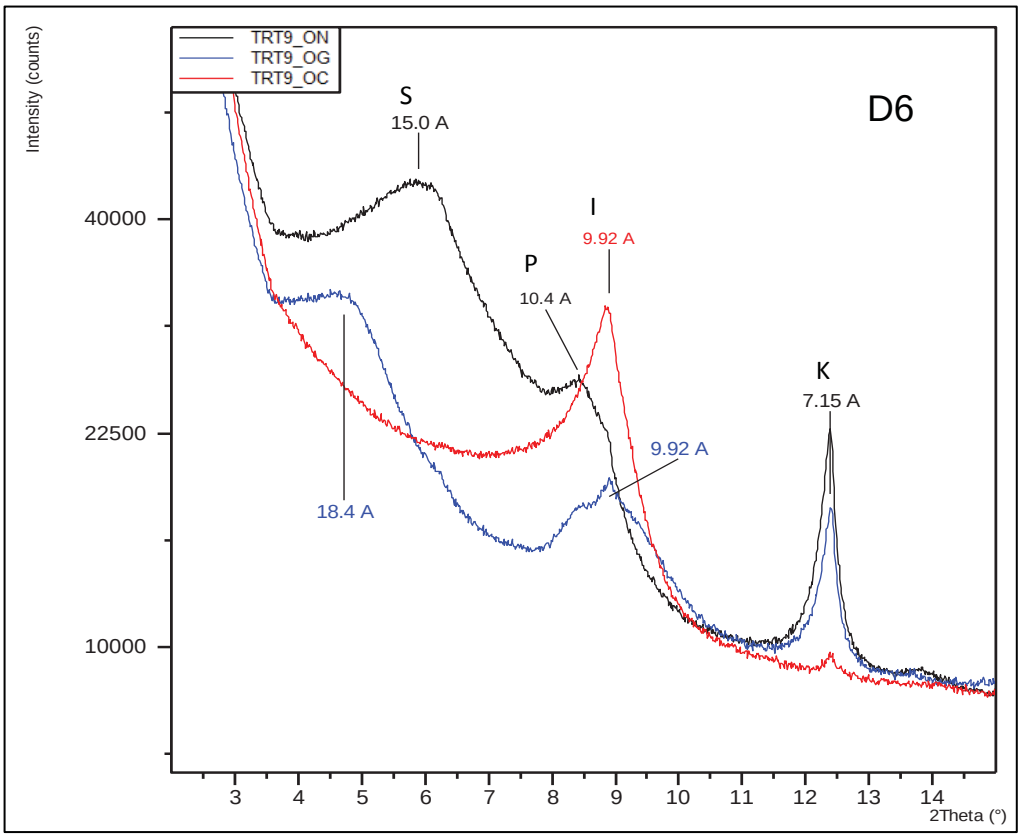


XRD of D6 layer of section D

**Figure S7.** K: Kaolinite; I: Illite; P: Palygorskite; S: Smectite; C: Chlorite

X-ray diffraction of clay coatings of section C level C2 and section D level D6.
in black: oriented clays, blue: glycol treated, red: heated.
C: chlorite; I: illite; K: kaolinite; P: palygorskite; S: smectite.

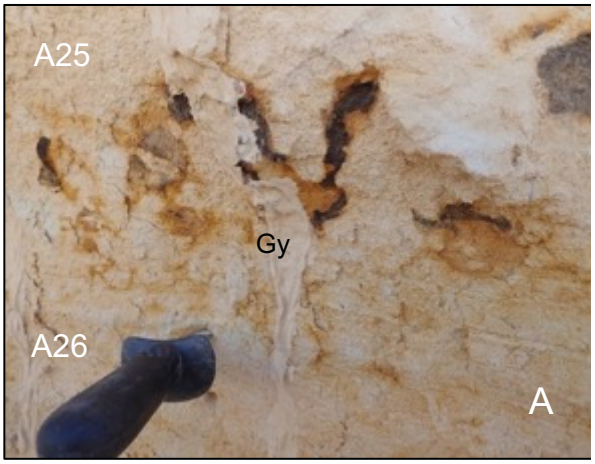


A) Detail of excavated Spring mound TRT36 section A, Manganese and iron oxides as a wavy boundary between layers A26 and A25.

Dissolved gypsum from the top of the mound precipitated as a thin pink coating of gypsum (Gy)


B) Detail of excavated Spring mound Guettaïa. TRT22 (33°40'39 N - 08°52'14 E)

Gypsum indurated layer at the top of the mound Horizontal redoxymorphic layers (gleyic and stagnic) at the top of the section.

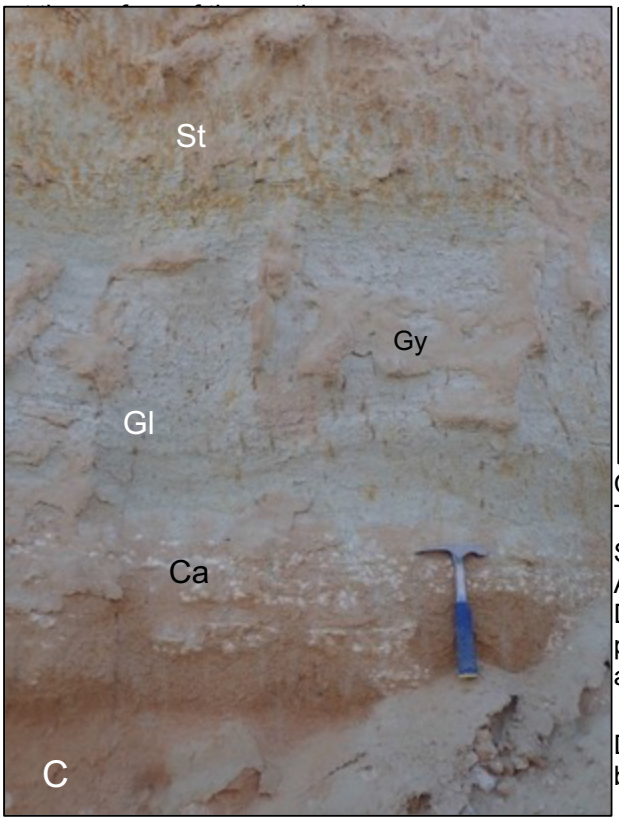



C) Detail of excavated Spring mound Guettaïa – TRT22 (33°40'39 N - 08°52'14 E)

Stagnic layer (St): Gleyic layer (Gl)
Aligned soft nodules of Calcium carbonate (Ca).
Dissolved gypsum from the top of the mound precipitated as a thin pink coating of gypsum(Gy) at the surface of the section.

D) Gypsum crust at the surface of Profile D. The basin is at the left of the photograph

**Figure S8.** Detailed photographs from different sections: A and B) occurrence of gleyic and or stagnic pedological processes in the sediments; C) Iron And Manganese oxide accumulation; D) gypsum crust at the top of section D.